

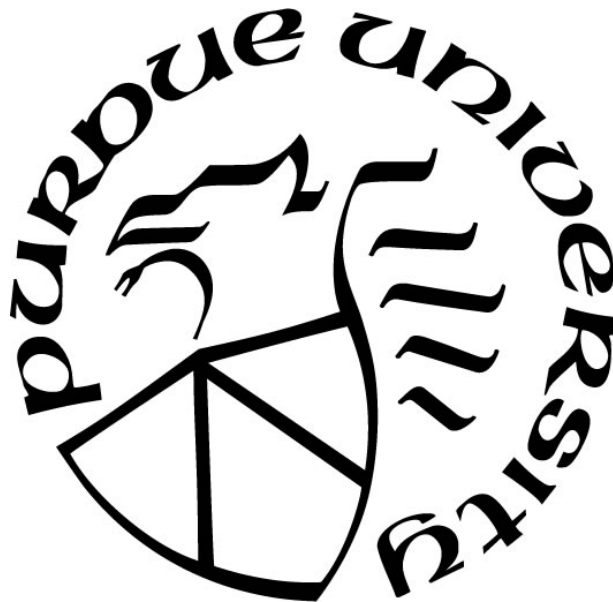
**LIQUID NITRATE FERTILIZER PRODUCTION WITH VARIOUS  
ATMOSPHERIC PRESSURE DISCHARGES**

by  
**Zhenyu Shen**

**A Thesis**

*Submitted to the Faculty of Purdue University  
In Partial Fulfillment of the Requirements for the degree of*

**Master of Science in Aeronautics and Astronautics**



School of Aeronautics & Astronautics

West Lafayette, Indiana

May 2019

**THE PURDUE UNIVERSITY GRADUATE SCHOOL  
STATEMENT OF COMMITTEE APPROVAL**

Prof. Sergey O. Macheret, Chair  
School of Aeronautics and Astronautics

Prof. Alexey Shashurin  
School of Aeronautics and Astronautics

Prof. Sally P. Bane  
School of Aeronautics and Astronautics

**Approved by:**

Prof. Weinong Wayne Chen  
Head of the Graduate Program

*This work is dedicated to my dearest mom, who pushed me to survive through the hardest time in my life and persuaded me to achieve more, even though I was starting out far behind the other children. With your unconditional love, I am always the invincible boy.*

## ACKNOWLEDGMENTS

I would like to thank my major Professor Sergey O. Macheret for providing me with a wealth of opportunities at Purdue University. He introduced me into the world of plasma and encouraged me to always strive for the best. The support and care he offered during my convalescence were priceless. He has always been a great mentor and made my graduate life here, at Purdue, unforgettable.

I would like to thank Dr. Andrei Khomenko for his feedback to my work, cooperation and of course friendship. He has always been the person who sobers me up. His patience helped me break through all the difficulties. In addition, I would like to express my gratitude to Mr. Vladlen A. Podolsky. His suggestions influenced me a lot, not only on my study, but also my future life.

Nevertheless, I am also grateful to my grandparents, Mr. Ximing Wang and Mrs. Shufan Liu for their love and every single phone call in which they showed me their care.

Last but not least, I would like to thank Miss Disi Zhang. You are the light of my life.

## TABLE OF CONTENTS

ACKNOWLEDGMENTS .....	4
TABLE OF CONTENTS.....	5
LIST OF TABLES .....	8
LIST OF FIGURES .....	9
ABSTRACT.....	12
CHAPTER 1. INTRODUCTION .....	13
1.1 The Haber-Bosch process and its alternatives .....	13
1.2 High temperature arc discharges.....	14
1.3 ‘Corona like’ discharges .....	15
1.4 Dielectric barrier discharges .....	16
1.5 PR and pulsed RF discharges.....	18
CHAPTER 2. MATERIALS AND METHODS.....	20
2.1 Atmospheric pressure high temperature arc plasma system .....	20
2.2 Atmospheric pressure DC positive corona discharge system .....	21
2.3 DC voltage driven cold plasma torch operating with helium .....	23
2.4 Atmospheric pressure dielectric barrier discharge system.....	24
2.5 Atmospheric pressure radio frequency plasma system.....	26
2.6 Dissolved species concentration measurements - water analysis .....	28
2.7 Reaction kinetics analysis - optical emission spectroscopy.....	30
CHAPTER 3. CALCULATION, RESULTS, AND DISCUSSION.....	33
3.1 Calculation of energy consumption per one nitrate ion .....	33

3.2	Calculation of different temperatures of DBD and RF plasma.....	33
3.3	Atmospheric pressure high temperature arc plasma .....	35
3.3.1	Plasma treatment, power, and current and voltage measurements .....	35
3.3.2	Water analysis.....	37
3.4	Atmospheric pressure DC positive corona discharge .....	40
3.4.1	Plasma treatment, power, and current and voltage measurements .....	40
3.4.2	Water analysis.....	41
3.5	DC voltage driven cold plasma torch operating with helium .....	43
3.5.1	Plasma treatment, power, and current and voltage measurements .....	43
3.5.2	Water analysis.....	45
3.6	Atmospheric pressure dielectric barrier discharge.....	47
3.6.1	Plasma treatment, power, and current and voltage measurements .....	47
3.6.2	Water analysis.....	47
3.6.3	Optical emission spectroscopy .....	52
3.6.4	DBD temperatures calculation and possible reaction kinetics .....	58
3.7	Atmospheric pressure radio frequency plasma .....	60
3.7.1	Plasma treatment, power, and current and voltage measurements .....	60
3.7.2	Water analysis.....	61
3.7.3	Optical emission spectroscopy .....	62
3.7.4	RF plasma temperatures calculation and possible reaction kinetics.....	67
CHAPTER 4. CONCLUSIONS AND FUTURE WORKS .....		69
4.1	Summary of all experiment results .....	69
4.2	Atmospheric pressure high temperature arc plasma system .....	70

4.3 Atmospheric pressure DC positive corona discharge .....	71
4.4 DC voltage driven cold plasma torch operating with helium .....	71
4.5 Atmospheric pressure dielectric barrier discharge system.....	71
4.6 Atmospheric pressure radio frequency plasma system.....	72
4.7 Future works .....	72
REFERENCES .....	74

## LIST OF TABLES

Table 3.1: “Raw” and calculated high voltage side average power.....	37
Table 3.2: Water parameters after 18-hour standing time. ....	39
Table 3.3: Energy costs per one nitrate/nitrite ion for high temperature plasma arc.....	40
Table 3.4: Energy costs per ion for atmospheric pressure positive DC corona discharge.....	43
Table 3.5: Energy costs per one nitrogen ion in Helium plasma torch treatment process.....	46
Table 3.6: Emission lines’ wavelength and their corresponding systems. ....	53
Table 3.7: Three temperatures under different PRFs.....	58
Table 3.8: Reaction kinetics at different pulse repetition frequencies.....	59
Table 3.9: Three temperatures under different experiment setups. ....	67
Table 4.1: Summary of results for all plasma sources and comparison with two water sources..	70
Table 4.2: Estimation for solar powered local fertilizer production factory located in Kenya. ...	73

## LIST OF FIGURES

Figure 2.1: The electrical scheme of arc discharge system. ....	20
Figure 2.2: The current shunt (the high precision 0.1 Ohm 1% resistor) calibration graph. ....	21
Figure 2.3: The electrical scheme for corona discharge system. The modification with a metal mesh displayed separately on the right.....	22
Figure 2.4: The current shunt (the high precision 4.7 kOhm 1% resistor) calibration graph. ....	23
Figure 2.5: The electrical scheme of helium plasma torch system. ....	24
Figure 2.6: Schematic of DBD plasma nitrate synthesis system. ....	25
Figure 2.7: Design of the custom tubular DBD cell. ....	25
Figure 2.8: Schematic of the electrical measuring system.....	26
Figure 2.9: Schematic of RF plasma nitrate synthesis system.....	28
Figure 2.10: Custom air core resonance high voltage transformer. ....	28
Figure 2.11: Dissolved species concentration measurement scheme. ....	29
Figure 2.12: Schematic of the optical emission spectroscopy setup for DBD plasma system. ....	31
Figure 2.13: Schematic of the optical emission spectroscopy setup for RF plasma system.....	31
Figure 3.1: Slit function for spectrometer with 100 $\mu\text{m}$ slit setting.....	35
Figure 3.2: Voltage and current profiles of plasma. Different time periods are shown: (0-10) s - left, (20-30) s – bottom center, (40-50) s - right. ....	36
Figure 3.3: Water analysis for atmospheric pressure high temperature arc discharge: pH - up left, conductivity - up right, peroxide concentration - middle left, nitrate concentration - middle right, and nitrite concentration - bottom.....	38
Figure 3.4: Current through a corona discharge. Overview on the left and one pulse zoom on the right. ....	40

Figure 3.5: Water analysis for atmospheric pressure DC positive corona discharge: pH - up left, conductivity - up right, peroxide concentration - middle left, nitrate concentration - middle right, and nitrite concentration - bottom.....	42
Figure 3.6: Current through a Helium plasma torch. Overview on the top left and one pulse zoom on the top right. The bottom graph shows the permanent DC current component. ....	44
Figure 3.7: Water analysis for DC voltage driven cold plasma torch: pH - up left, conductivity - up right, peroxide concentration - middle left, nitrate concentration - middle right, and nitrite concentration - bottom. ....	46
Figure 3.8: Voltage and current profiles (left) and energy per pulse (right).....	47
Figure 3.9: Water analysis for 500Hz-frequency DBD treatment in 500 mL water: pH - up left, conductivity - up right, peroxide concentration - middle left, nitrate concentration - middle right, and nitrite concentration - bottom. ....	49
Figure 3.10: Comparison between 500 Hz- and 2000 Hz-frequency DBD treatment in 500 mL water: pH - up left, conductivity - up right, peroxide concentration - middle left, nitrate concentration - middle right, and nitrite concentration - bottom. ....	50
Figure 3.11: Nitrite concentration for different DBD pulse repetition frequencies in 10 mL water tank.....	51
Figure 3.12: Nitrate energy costs versus pulse repetition frequency in three systems. ....	52
Figure 3.13: Spectrums for DBD with different pulse repetition frequencies (from top to bottom: 30 Hz, 100 Hz, 200 Hz, 500 Hz, and 2000 Hz). ....	54
Figure 3.14: Second order diffraction test for DBD with different pulse repetition frequencies (from top to bottom and from left to right: 30 Hz, 100 Hz, 200 Hz, 500 Hz, and 2000 Hz).....	57
Figure 3.15: Voltage and current profiles (left) and energy per pulse (right) on LV side of the plasma. ....	61
Figure 3.16: Water analysis for RF plasma treatment with 4 L water: pH - up left, conductivity - up right, peroxide concentration - middle left, nitrate concentration - middle right, and nitrite concentration - bottom. ....	62

Figure 3.17: Spectrums for RF plasma with different experiment setups (from top to bottom and from left to right: no air flow and no water spray, only fresh air in and no water spray, full air circulation and no water spray, full air circulation and water spray, and only fresh air in, water spray, and opened lid). ..... 64

## ABSTRACT

Author: Shen, Zhenyu. MS

Institution: Purdue University

Degree Received: May 2019

Title: Liquid Nitrate Fertilizer Production with Various Atmospheric Pressure Discharges

Committee Chair: Sergey O. Macheret

Plasmas can be used to increase the probability of maturity of seeds and disinfect them. The water applied on plants can also be treated with plasma to reduce bacteria. Discharges normally used to treat water including dielectric barrier discharges, gliding arcs, DC, AC, or pulsed coronas, and various direct discharges in liquid. After treatments, reactive oxygen (ozone) and nitrogen species (nitrite and nitrate) will appear in the water solution. Then, by applied this water, the lifecycle of plant could be significantly influenced. Plasma has a great potential to play an important role in the agriculture discipline. The process of synthesizing nitrate fertilizer with water, air, and electric spark has been known for a long time. But due to low nitrate yield and high energy consumption, it was replaced by the Haber-Bosch process in the first half of the 20<sup>th</sup> century. The Haber-Bosch process, however, has several disadvantages: it requires natural gas as a raw material, fixes nitrogen in the form of ammonia, and generates oxycarbides as byproducts. Thus, the concept of manufacturing nitrogen fertilizer with only water, air and electricity is still appealing.

In this project, we want to measure the pH value and conductivity of the water treated by various atmospheric pressure discharges including the arc discharge, DC positive corona discharge, DC voltage driven cold plasma torch operating with helium, dielectric barrier discharge (DBD), and radio-frequency (RF) plasma. Also, it is necessary to verify the existence of different important species in the treated water such as peroxide, nitrite, and nitrate ions by measuring their concentrations. Based on current and voltage measurements and wall-plug electrical energy consumption, energy efficiency of nitrate synthesis was determined in these five plasma systems. Optical emission spectroscopy was employed to study the reaction kinetics of both DBD and RF discharge. Our goal is to produce enough nitrate ions, by plasma treatment with minimal energy input (the value should be at least close to the Haber-Bosch process), in water which could be further used as fertilizers.

## CHAPTER 1. INTRODUCTION

### 1.1 The Haber-Bosch process and its alternatives

The Haber-Bosch process, also known as the Haber process, artificially fixes nitrogen to produce ammonia by a reaction with hydrogen using metal catalysts. This chemical reaction requires high temperatures and pressures conditions.<sup>1</sup> The Harbor process is very efficient and the energy consumption per one nitrogen oxide or ammonia molecule is between 5-12 eV. This process is widely employed in the fertilizer manufacture and produces more than 450 million tons of nitrogen fertilizer per year. However, natural gas, as a raw material, is a requisite. As a result, around 40% of the world's natural gas production, which is equal to 1-2% of the total world energy supply, is consumed in the Haber process.<sup>2,3,4,5</sup> In addition, a large amount of CO<sub>2</sub> (around 300 million metric tons) is emitted which contributes a lot to the global warming.<sup>6</sup> Thus, any improvement in the Harbor process will lead to dramatical changes in the situation of environment and benefit the economy. The International Energy Agency (IEA) lists ammonia as the molecule with the greatest potential to increase energy efficiency and reduce greenhouse gases (GHG) emissions by 2050 with new catalytic process.<sup>7</sup> Furthermore, the background of world generated with renewable energy, the demand of localized fertilizer production<sup>8</sup> and findings of new applications for nitrogen species<sup>9</sup> requires novel methods to fix nitrogen atoms in the form of NO<sub>x</sub> or NH<sub>3</sub>.

Fertilizer produced by interactions between plasmas and water is considered to be attractive due to its potential to achieve even higher energy efficiency. Currently, plasmas play an important role in the agriculture. They can be used to increase the probability of maturity of seeds and disinfect them. The water applied on plants can also be treated with plasma to reduce bacteria.<sup>10,11</sup> Discharges normally used to treat water including dielectric barrier discharges,<sup>12</sup> gliding arcs,<sup>13</sup> DC, AC, or pulsed coronas,<sup>14,15,16</sup> and various direct discharges in liquid.<sup>17</sup> After treatments, reactive oxygen (ozone) and nitrogen species (nitrite and nitrate) will appear in the water solution. Then, by applied this water, the lifecycle of plant could be significantly influenced.<sup>19</sup> Plasma has a great potential to play an important role in the agriculture discipline. At Purdue University, low-temperature plasma even plays a role in direct olive oil analysis.<sup>20</sup>

## 1.2 High temperature arc discharges

In general, the operation frequencies of pulsed arc systems are between  $10^{-2}$ - $10^{-3}$  Hz, and the maximum current will exceed one thousand amperes with a voltage rise in an order of microsecond. The peak voltage is around 1 to 10 kV. What appears is that strong shock waves will be generated inside the cavitation zone by the arc, and air bubbles will be produced. Gases inside these bubbles will be ionized and we call them plasma bubbles. The duration of peaks of the magnitude of UV emission and concentration of radicals are determined to be short in this cavitation zone.<sup>21</sup>

Vanraes mentioned that gliding arc discharges above a water surface was a popular approach for water treatment with plasma.<sup>22</sup> For his specific discharge, two electrodes of which the separation distance is diverging are placed above a water solution. According to the authors' description, an electric arc forms at the shortest electrode gap. Then it glides along the electrode's central axis pushed by a gas flow whose direction is pointing at the water surface.

Besides Vanraes's introduction to gliding arc discharges, Malik described the mechanics of arc formation on a more universal level.<sup>23</sup> The chemical reaction kinetics for nitric oxide generation in arc discharges are also mentioned in detail. This article provides important information about how different oxynitride is transformed to each other in arc discharges.

Several scientists employed arc discharges to do water treatments and then apply this water to plants. Park et al discussed how the water, treated with different atmospheric discharges, would influence the germination, growth rates, and overall nutritional value of various plants.<sup>24</sup> In this article, they reported experiments with three kinds of discharges: thermal spark discharge, gliding arc discharge, and transferred arc discharge. Non-thermal gliding arc discharge plasma results in productions of a large amount of peroxide ions and acidoid. Gliding arc discharge also makes the pH value of treated water drop, but the production of peroxide ions are replaced by that of the reactive nitrogen species, including nitric oxide, nitrite ions, and nitrate ions. Based on the initial water compositions, Spark discharge treatment could increase the pH value of treated water to be neutral or alkaline. Again, reactive nitrogen species will be produced. Besides, the authors

mentioned that the peroxide ions and reactive nitrogen species are not stable and will be consumed quickly. For this reason, special storage methods need to be developed.

Later, in 2018, Patil et al proposed the use of pulsed gliding arc discharge to produce nitrogen oxide.<sup>25</sup> He threw out the idea to build a closed system to produce liquid fertilizer. To summarize, the authors suggested that the initial fraction of oxygen should be around 40-48% for best performance and that will lead to an enhancement of 11 % in NO<sub>x</sub> production. It is intuitive that longer residence time in the gliding arc chamber will increase the concentration of reactive nitrogen species. Lower flow rate will help extend the residence time and thus, improve the productivity of those species. The author also pointed out that the appearance of argon and increased temperatures of the initial gas flow will make the energy efficiency drop.

### 1.3 'Corona like' discharges

We built our second device with the atmospheric pressure D.C. positive corona discharge. Compared with typical arc discharges, the pulsed corona system operates at higher frequencies: 10<sup>2</sup> to 10<sup>3</sup> Hz and the maximum current never exceeds 100 A. Basically, the peak duration of voltage is on the order of several nanoseconds. Normally, a streamer-like corona generated in water accompanies with relatively weak shock waves. What appears is that weak-to-moderate ultraviolet radiation is formed, and a moderate amount of bubbles is observed. There are radicals and reactive species formed near the high voltage electrodes. Compared with the pulsed arc discharge, this type of discharge is more sensitive to the solution conductivity.<sup>21</sup>

The properties of corona discharges are also reviewed in Goldman's article.<sup>26</sup> The emphasis of this paper is on the features that make corona discharges unique for building non-equilibrium chemical reactors, including their stability, flexible choices of various gases, and convenience of operation over a wide range of pressure, especially the atmospheric pressure. Also, Goldman discussed the present and proposed applications. Corona discharges could be used to synthesize ozone and ammonia. Normally, the streamer type coronas are employed for the generation of ozone. Air or oxygen will fill the gap where one of the electrodes is covered with an insulating layer to prevent

streamer-arc transition. Besides, the writer stressed that the efficiency of this synthesis process is quite low (around 2%) and further research efforts are needed.

In Clements's study, he analyzed both the chemical and physical factors that occurred when both electrodes were immersed, and the pulsed corona discharges was generated in water. He used the point-to-plane geometry (the discharge is ignited between the stud high voltage electrode and metal sheet).<sup>27</sup> Lisitsyn have also reported a liquid-phase pulsed electrical discharge reactor in which the disk-shaped electrode is placed in a ring-to-cylinder configuration.<sup>21</sup> In addition, Brisset et al published two articles with corona discharges experiments.<sup>28,29</sup> The first one investigates the interaction between an air plasma and water: an atmospheric pressure DC corona discharge with point-to-plane configuration. After the plasma treatment, acidoid is produced inside the solutions. Besides, they used a custom tool to measure the treated area. They suggested that this area depended on voltage and current magnitude, on the distance between the point electrode and the plane one, and on the acidity of the initial water. Five years later, the second one was done. They continued their research in the aqueous solutions treated by the same discharge and found out that air is enriched with  $\text{NO}_2^-$  and  $\text{NO}_3^-$ . They commented that the nitrate concentration successively increased with the treatment time while that of the nitrites presented a maximum. Also, both concentrations increased with the current magnitude and the treatment time. In addition, they suggested a series of reactions that resulted in the production of nitrate species which will be an important reference for our future work on the study of reaction kinetics.

#### 1.4 Dielectric barrier discharges

Gibalov introduced two kinds of configurations of dielectric barrier discharges - the gas gap type and the surface type in 2000.<sup>30</sup> For both types, a dielectric layer is put between two conducting electrodes. The gas gap type DBD is normally with a volume discharge arrangement while the surface type features in an arrangement with a surface electrode on a dielectric layer and an the other one on its reverse side. For the first one, several micro discharges will form inside the gas gaps at atmospheric pressure. For the surface type, multiple discharge steps are observed. The author mentioned that the applied voltage determined the number of micro discharges and steps.

Several researchers implement DBD to produce different chemical species in water. Shainsky et al have employed this plasma source to treat water in 2012.<sup>31</sup> It was demonstrated that a strong oxidizer will appear in the distilled water treated with DBD plasmas. The pH value is below 7. Their study is aimed to find out which acid oxidizer is created in water by DBD plasma treatment. They confirmed the presence of nitric acid in the water treated with DBD. Besides, the article also purposes that the superoxide anion should be responsible for the water acidity. The water treated by the DBD plasma remained stable for at least a day. In addition, they suggested a series of reactions that resulted in the production of peroxide species. In the end, they purposed the usage of this kind of treated water-the food sterilization. Dockery et al. study the surface acid chemistry associated with DBD treatment of polyethylene.<sup>32</sup> They changed the operating parameters of the DBD including dose, humidity, airflow, electrode gap and electrode configurations. All of these are proved to influence the production of acids on the polyethylene surface. They also suggested that the formation of nitric acids is due to reactions between nitrogen species and hydroxyl radicals in the gas phase. Elsaadany et al also did a research with the DBD plasma.<sup>33</sup> They conducted a study that aimed at investigating whether nitric oxide generated using DBD plasma could mediate osteoblastic differentiation of osteoprogenitor cells without creating toxicity. Heuer et al. showed that DBD generated above skin would produce several reactive nitrogen species including nitric oxide.<sup>34</sup> The produced nitric oxide may be used to disinfect and heal wound. Laurita et al. analyzed the reactive species in the water treated by nanosecond pulsed DBD air plasma.<sup>35</sup> Phenol was used as chemical probe for reactive oxygen and nitrogen species.  $H_2O_2$ ,  $NO_3^-$  and  $NO_2^-$  concentrations were measured. Besides, they determined the change of pH and conductivity of the treated water and studied the post discharge kinetics of reactive species with the help of the phenol.

On the contrary, some scientists purpose taking advantage of new species created during plasma treatment to degrade unwanted ingredients in the water solution. Hu et al. purposed using DBD plasma for degradation of dimethoate in aqueous solution.<sup>36</sup> Besides, Feng et al. purposed a dielectric barrier discharge plasma reactor for degradation of aqueous 3,4-dichloroaniline in 2014.<sup>37</sup> Marotta et al. talked about the advanced oxidation process for degradation of aqueous phenol in a DBD reactor.<sup>38</sup>

## 1.5 PR and pulsed RF discharges

Schutze et al. gave a review of the development of the atmospheric-pressure plasma jet in 1998. This discharge is ignited by applying the 13.56 MHz radio frequency power to the inner electrode. The applied voltage can range from 100 to 250 V. A gas flow, which consists of helium, oxygen, and other gases, passes through the interval between the two concentric electrodes. For this specific jet, it has a temperature between 25-200 °C with electron and ion densities of  $10^{11}$ - $10^{12}$  cm<sup>-3</sup>. One desired feature is that the reactive oxygen and nitrogen species are in high concentrations.<sup>39</sup>

Park et al. developed an atmospheric pressure plasma source generated by radio frequency power in 2000.<sup>40</sup> This discharge is homogeneous and stable with a gas temperature lower than 300 °C. The volume of this discharge is a constant. A large amount of reactive oxygen species is produced along with this discharge. The authors concluded that the jet can remain a nonequilibrium characteristic during the production of chemically active species.

Moon et al. discussed an atmospheric pressure RF glow discharge in 2004.<sup>41</sup> It is ignited with a 13.56 MHz RF power supply and assisted with argon feeding gas. The plasma region size is 200 mm × 50 mm × 5 mm. During operations, the length of the plasma could be up to 400 mm. The rotational temperatures and vibrational temperatures fall in the range of 490 to 630 K and 2000 to 3300 K, respectively. Balcon et al. did a further investigation in this RF plasma.<sup>42</sup> Two different discharge regimes could be ignited by changing the pulse parameters. They showed that pulse periods less than 100 μs will lead to a filamentary discharge while 1 ms period or longer will result in a glow discharge. The electron temperature is 1.3 eV for the glow discharge and 1.7 eV for the filamentary discharge. Besides, an estimate of electron temperature was approximately 1.3 eV for the glow mode and 1.7 eV for the filaments.

Smith et al. talked about the breakdown behavior in RF argon discharges.<sup>43</sup> They measured the breakdown voltage and determined the shape of the Paschen curve. The Paschen minimum occurs when the applied voltage is 70 V and the pd value is equal to 0.3 mTorr·cm. They concluded that both voltage and pd value required for breakdown in RF systems are much lower than those in DC systems. For DC discharges, electrode material determines the features of the Paschen curve. As

for RF discharges, only left-hand side of the Paschen curve is influenced by the electrode material, excluding the minimum point.

Jeong et al. used a RF plasma jet to etch materials.<sup>44</sup> Again, this jet is driven by a 13.56 MHz radio frequency power. The maximum power applied to the high voltage electrode is 500 W. The temperature of the gas, which is a mixture of helium, oxygen and carbon tetrafluoride, is around 200°C. It flows between the outer grounded and central high voltage electrodes. Babayan et al. used the atmospheric pressure plasma jet to do deposition of silicon dioxide films.<sup>45</sup> Zajickova et al. conducted a study of plasma polymerization from acetylene in pulsed RF discharges.<sup>46</sup> Benedictis et al. employed time resolved optical diagnostics to study energy transfers in N<sub>2</sub>/O<sub>2</sub> pulsed RF discharges.<sup>47</sup> The relaxation mechanisms are well summarized in this article. Specially, the authors mentioned that, during the discharge, the density of low energy electrons were strongly reduced with the O<sub>2</sub> addition.

Through this thesis, we systematically unravel plasma-assisted nitrate production at atmospheric pressure in various discharge systems, including high temperature arc discharge, DC positive corona discharge, DC voltage driven cold plasma torch operating with helium, DBD, and RF plasma, aiming at a lower energy consumption process for plasma-assisted fertilizer production. Here, we measured pH value, conductivity, and concentrations of peroxide, nitrite, and nitrate of water treated by those discharges. With current and voltage profiles, we further calculated the energy consumption per one nitrate ion. We also employed the optical emission spectroscopy to study the reaction kinetics and calculate electron temperature, rotational temperature, and vibrational temperature for DBD at different pulse repetition frequency (PRF) and RF plasma with different experimental setups. Finally, a kinetic scheme of plasma-assisted nitrate synthesis in a DBD cell and RF discharge chamber is postulated.

## CHAPTER 2. MATERIALS AND METHODS

### 2.1 Atmospheric pressure high temperature arc plasma system

The atmospheric pressure arc plasma system consists of a high voltage 60 Hz transformer, a powermeter, current and voltage probes connected to the oscilloscope, and two graphite electrodes: as shown at Figure 2.1. The transformer's low voltage coil is connected to a common power plug, with 120 V voltage and 60 Hz frequency, through the power meter (WT210, Yokogawa), which allows us to measure the "raw" electricity consumption (how much total power we have deposited into the whole system). A high voltage oscilloscope probe PPE 6 kV (LeCroy) is connected directly to the high voltage coil of the transformer for measuring voltage of plasma. The current is metered by a shunt - a high precision 0.1 Ohm 1% resistor (RS-5, Dale). To provide even better accuracy, we also performed a current calibration of this component (presented at Figure 2.2). The calibration was carried out with the same value of current that drive the arc discharge in this experiment. The voltage drop on the shunt is around 0.2 V and it is negligible in comparison to almost 2 kV between the graphite electrodes. Both plasma voltage and current are acquired by a 3.5 GHz oscilloscope (WavePro 735Zi, LeCroy).

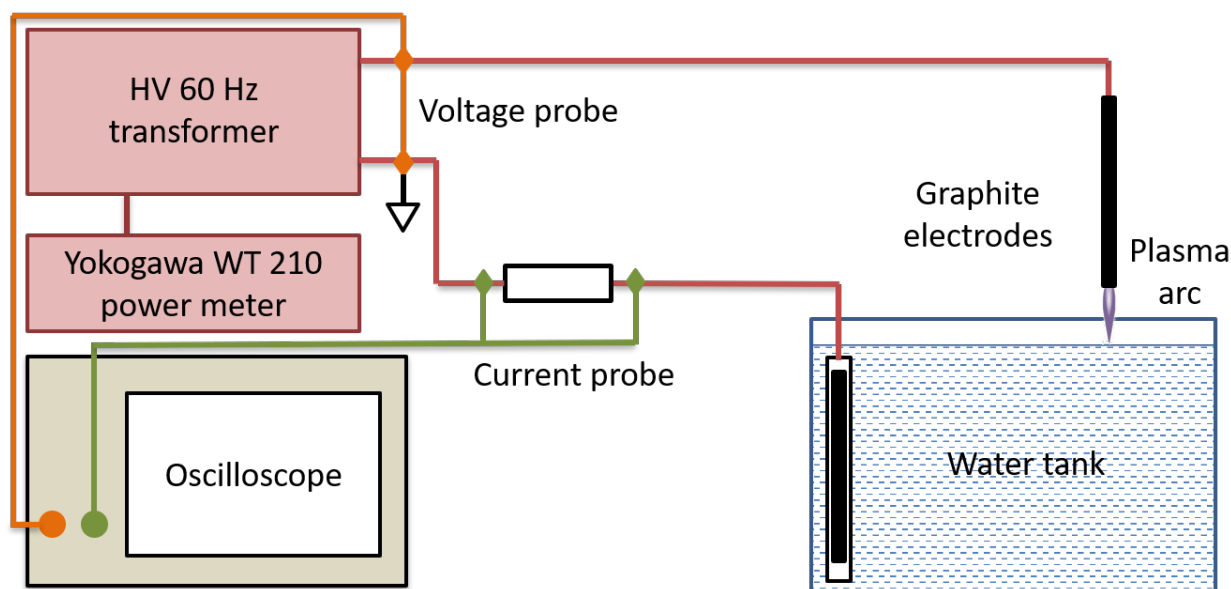


Figure 2.1: The electrical scheme of arc discharge system.

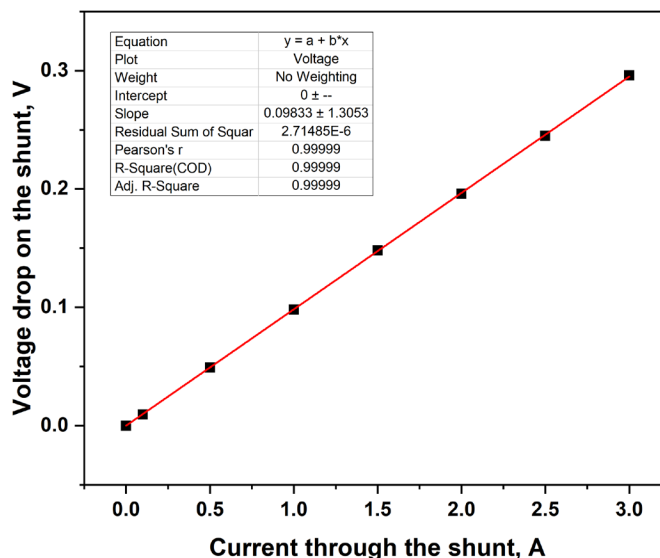


Figure 2.2: The current shunt (the high precision 0.1 Ohm 1% resistor) calibration graph.

Under this kind of electrical setup, all the plasma current went through the water under treatment and then, to the immersed electrode. To minimize the effect of electrolysis process between them, both electrodes are made from graphite. Furthermore, graphite is an ideal material to work with atmospheric pressure high temperature arc discharge since that high temperature will result in a rapid destruction on the electrodes. The grounded electrode of the transformer is submerged into water, as mentioned. To avoid appearance of an arc between it and the HV electrode, insulated rubber tape and thick PTFE tube are employed to cover the surface of the immersed electrode. The high voltage electrode is taped on a glass rod to prevent an accidental electric shock.

## 2.2 Atmospheric pressure DC positive corona discharge system

Atmospheric pressure DC positive corona discharge is usually conducted with tens of kilovolts applied voltage and several microamperes DC current. The configuration scheme for our corona discharge system is shown by Figure 2.3. It looks very similar to the previous one - the atmospheric pressure arc discharge system. Instead of 2 kV and 60 Hz high current power supply, we switched to an up-to-40 kV DC high voltage power supply - PS/EW40P15 (Glassman High Voltage Inc). Also, because of the change of the high voltage power supply which means the values of voltage and current on the plasma would change accordingly, we used different current and voltage probes:

a precision 4.7 kOhm resistor (1% accuracy, MS-260, Caddock Electronics Inc) serves as a current shunt and the voltage probe is directly integrated into the DC HV power supply. For better accuracy the shunt calibration is performed as well (Figure 2.4).

We replaced the material of the high voltage electrode from graphite to tungsten and sharpened the tip of it before the very first plasma ignition. We have designed two modifications of corona setups as shown in Figure 2.3: for the first one, a discharge occurs between the tungsten stud electrode and the water surface which means the plasma will interact with water directly (Figure 2.3, on the left); as for the second one, a handcrafted metal mesh will replace the graphite electrode. The plasma is ignited above this metal mesh which is placed at the top of the beaker that holds water (Figure 2.3, on the right). The distances between the pin of tungsten electrode to the water surface, for the first case, and the pin to the metal mesh, for the second case, are always 1 cm.

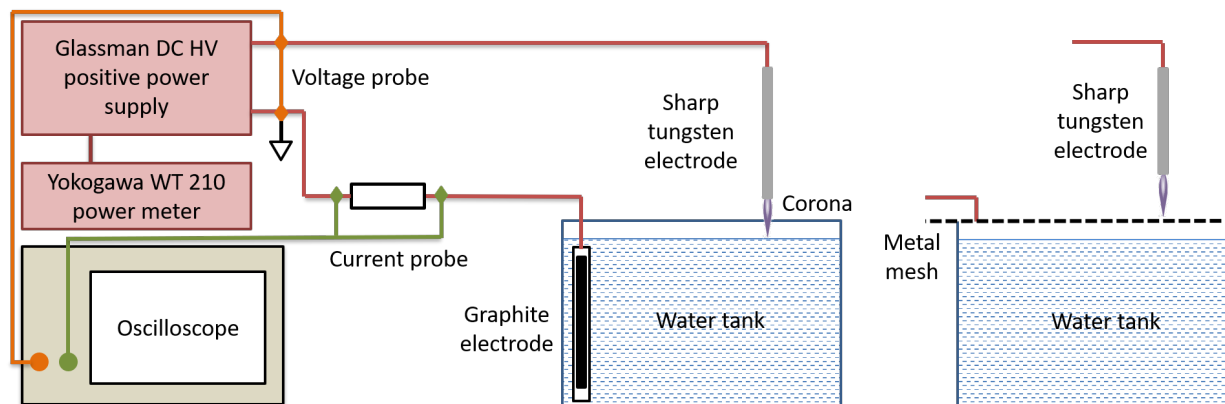


Figure 2.3: The electrical scheme for corona discharge system. The modification with a metal mesh displayed separately on the right.

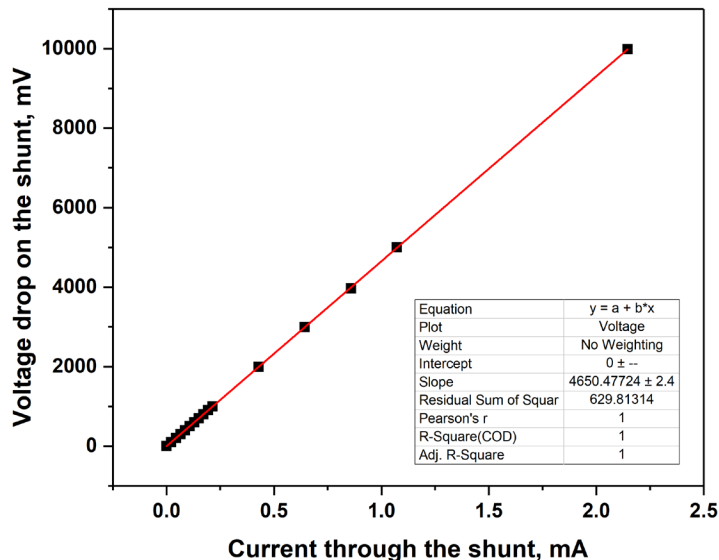


Figure 2.4: The current shunt (the high precision 4.7 kOhm 1% resistor) calibration graph.

### 2.3 DC voltage driven cold plasma torch operating with helium

The plasma gun was borrowed from Professor Alexey Shashurin's laboratory (Purdue, School of Aeronautics and Astronautics) This piece of equipment is well described in his article 'Study of atmospheric pressure plasma jet parameters generated by DC voltage driven cold plasma source'.<sup>48</sup> The electrical configuration scheme is shown by Figure 2.5. An up-to-5 kV DC high voltage is generated by a Bertan 225 power supply. The power source is connected to one end of a 10 kOhm resistor of which an oscilloscope probe is attached at the other end for the voltage measurement. The current flows through the central high voltage electrode of the plasma gun. The peripheral part of this gun (nozzle) is wrapped with a piece of copper foil and connected to a precision 4.7 kOhm resistor (1% accuracy, MS-260, Caddock Electronics Inc), which serves as a current shunt. Furthermore, the Yokogawa WT210 power meter is employed for the 'raw' power measurement. The distance between the outlet of the plasma gun and the water surface is 3 cm.

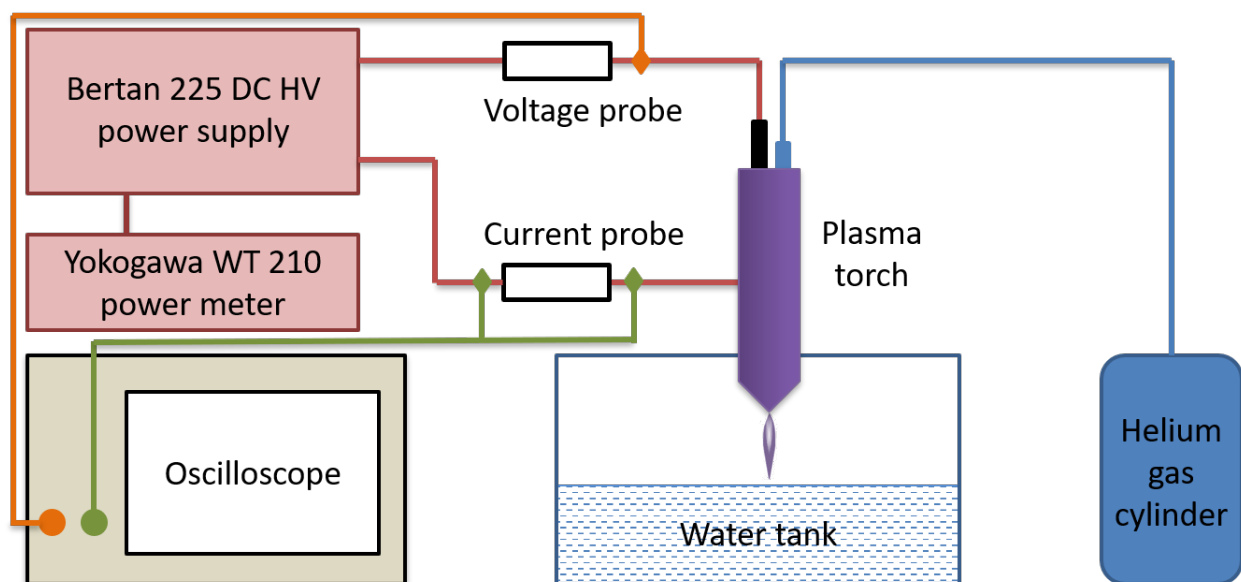


Figure 2.5: The electrical scheme of helium plasma torch system.

#### 2.4 Atmospheric pressure dielectric barrier discharge system

Figure 2.6 introduces the design of DBD plasma nitrate synthesis system. A radio frequency (RF) waveform generator 33622A (Keysight) provides the initial trigger signal. This signal, then, triggers a high voltage nanosecond pulse generator FPG 10-100MC2-10 (FID GmbH) whose positive output is connected to the HV electrode of the DBD cell by a 75 Ohm coaxial cable. A hose will guide the gas activated by plasma inside the cell into the water. A bubble diffuser air stone is mounted at the other side of the hose to increase contact surface between the plasma activated gas (PAG) and the water. Two water tanks with 10- and 500-mL distilled water respectively are prepared for different experimental sets. A PAG recirculation system is added to increase the productivity of nitrate ions. Fresh air is drawn out near the top of water surface and goes into the console-driven air pump (Masterflex). Then, it flows through the DBD cell. The flow rate is set to be 0.5 L/min and the total gas volume inside the PAG recirculation system is 50 mL.

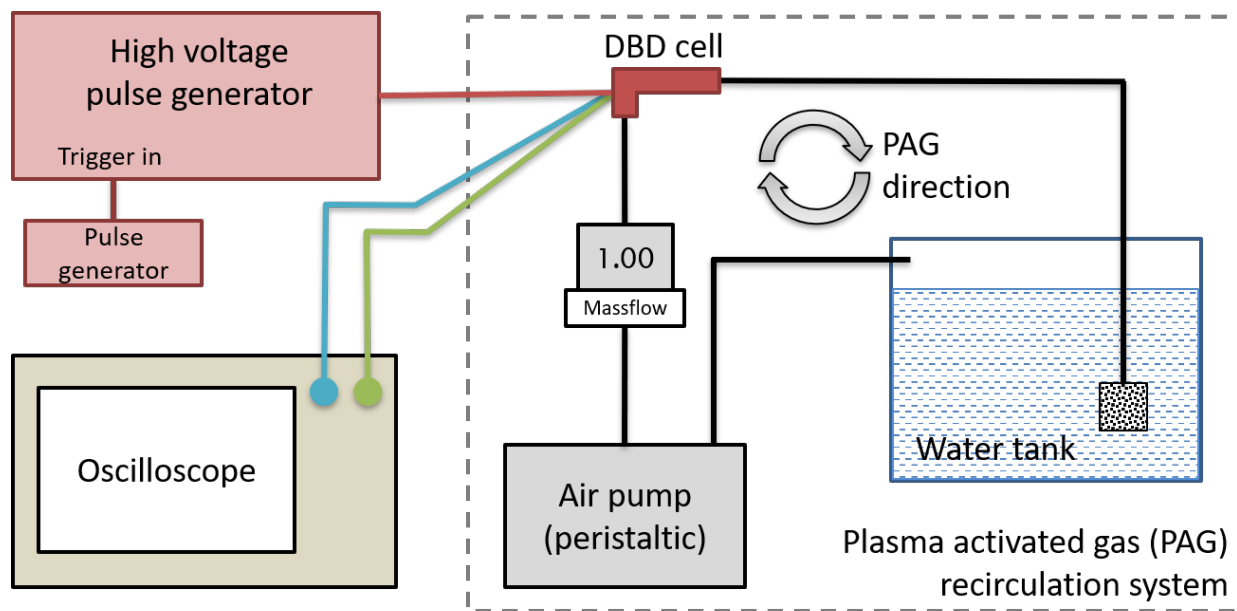


Figure 2.6: Schematic of DBD plasma nitrate synthesis system.

Plasma nitrate synthesis is performed in a DBD cell. This custom tubular cell is depicted in the Figure 2.7 and it consists of a central cylindrical copper electrode, peripheral glass tube, and outer grounded metal mesh by which the tube is wrapped. The center high-voltage electrode has a diameter of 1.4 mm. The tube's inner and outer diameters are 3.15 mm and 4.25 mm respectively which lead to a wall thickness of 0.55 mm.

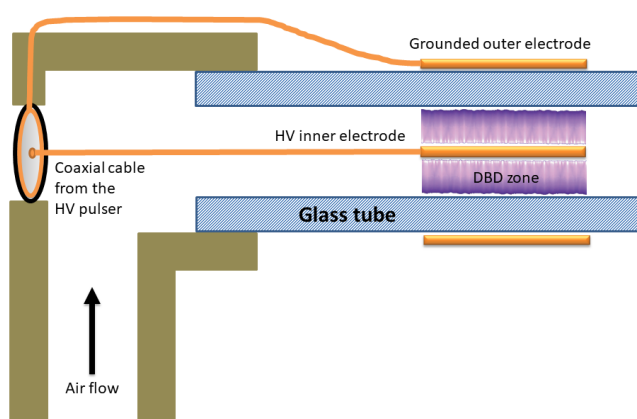


Figure 2.7: Design of the custom tubular DBD cell.

A 3.5 GHz oscilloscope - WavePro 735Zi (LeCroy) is employed to obtain the current and voltage profiles of the DBD plasma inside the cell. With these profiles, the power consumption of the plasma can be further calculated. Figure 2.8 shows details about how the oscilloscope is connected to the DBD plasma cell. A custom voltage probe and a current transformer (Bergoz fast current transformer) are used to measure voltage and current respectively. The voltage probe is made of a 4.7 kOhm high precision resistor (MS 260 series, Caddock, USA) and a 50 Ohm impedance coaxial cable. The length of coaxial cables for both probes should be the same to prevent additional time delay between the voltage and current profiles. 30 dB attenuators are mounted on both cables in case that the maximum voltage and current of plasma are far higher than the limits of the oscilloscope. For better accuracy, the voltage and current probes are placed as close as possible to the DBD cell. The ground of the oscilloscope is connected to the outer grounded metal mesh of the DBD cell.

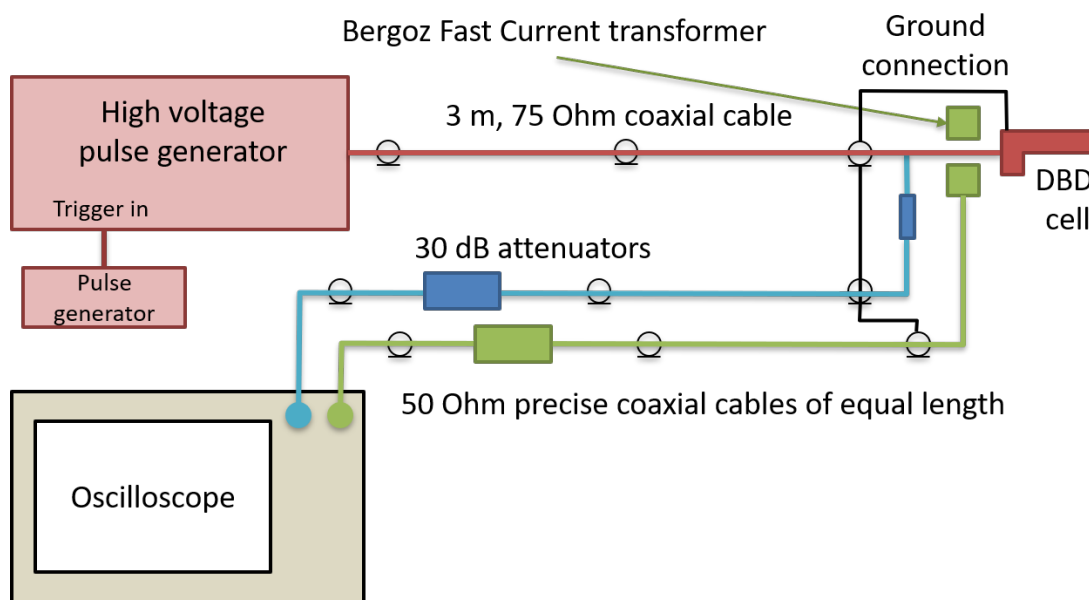


Figure 2.8: Schematic of the electrical measuring system.

## 2.5 Atmospheric pressure radio frequency plasma system

Figure 2.9 introduces the design of RF plasma nitrate synthesis system. A radio frequency (RF) waveform generator 33622A (Keysight) provides the initial RF signal. This signal, then, goes

through a high-power RF amplifier (AG 1012, T&C Power Conversion Inc.). The output signal will be sent to a custom air core resonance transformer (Figure 2.10). The RF plasma will be generated at the other end of the transformer where six thick copper wires are bonded together to play the role as a high voltage electrode. The volume of distilled water inside the tank for this system is 4 L. Like the DBD plasma nitrate synthesis system, a PAG recirculation system is added to increase the productivity of nitrate ions. Air is drawn out near the top of water surface and goes into a centrifugal air pump. Then, it flows back to the water tank. The flow rate is set to be 60-70 L/min and the total gas volume inside the PAG recirculation system is 12 L. A hose will lead water into a peristaltic pump (Masterflex). Several water spray heads are mounted on the back side of the tank's lid and they are connected to the hose. Then, water spray is formed to increase the contact area between the RF plasma and treated water. The set water flow rate is 2 mL/s. Besides, the same 3.5 GHz oscilloscope - WavePro 735Zi (LeCroy) is employed to obtain the current and voltage profiles of the RF plasma.

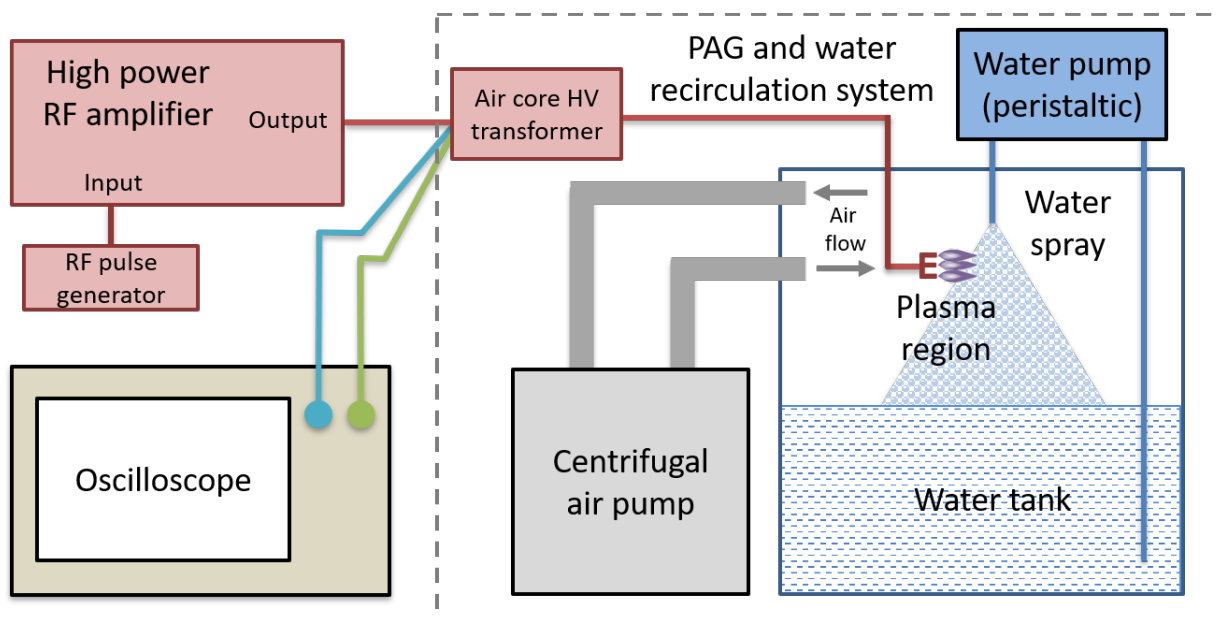


Figure 2.9: Schematic of RF plasma nitrate synthesis system.



Figure 2.10: Custom air core resonance high voltage transformer.

## 2.6 Dissolved species concentration measurements - water analysis

The measuring system consists of the main component - a multi-channel meter SevenExcellent (Mettler Toledo) and four different probes:

- pH electrode - InLab Routine Pro
- Conductivity electrode - InLab 731-ISM

- Ion selective electrode for nitrates - prefectION NO<sub>3</sub><sup>-</sup> combination
- Dissolved oxygen electrode - InLab OptiOx

All the probes are from Mettler Toledo. Temperature sensors go along with both the pH and conductivity electrode. To minimize the effect of uneven concentration distribution in water during measurements, a magnetic stirrer is used. This system is shown on Figure 2.11.

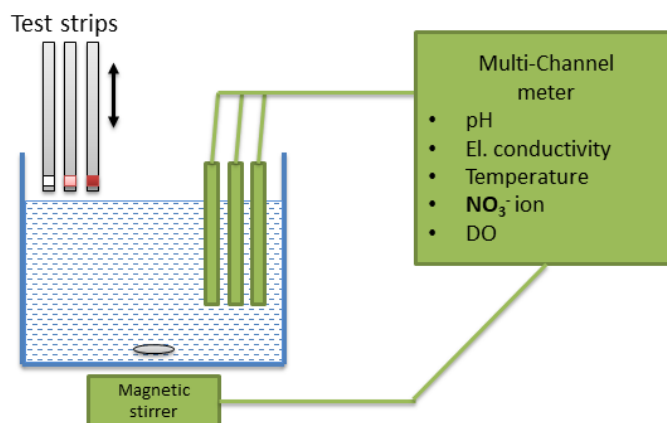


Figure 2.11: Dissolved species concentration measurement scheme.

The first step is to prepare the equipment which will be used during the water treatment and test process. This procedure is necessary because it can make sure that the result is accurate which means the result is not affected by residues on those equipment (the values of some species' concentrations are small and thus, could be seriously affected by these residues). To start with, the pH, conductivity, and peroxide, nitrite, and nitrate concentrations probes are thoroughly washed by distilled water. Then, the water will be wiped out by a piece of clean tissue. After that, the magnetic stirrer, tweezers and a glass rod are cleaned by the same distilled water and put into a clean beaker for future purposes. Some chemical properties of water after plasma treatment – peroxide, nitrite, and nitrate concentration - are investigated by using test strips 'MQuant' (Merck) at the same time which can serve as a proof to the result obtained by the multi-channel meter. The measuring procedures are executed exactly according to the manufacturer's instruction: dipping a strip in the water under investigation (the water should be in a certain temperature range or the error will be large), moving the strip toward described direction, waiting required period of time,

and visually comparing the color of the reacting zone to a color's scale provided with each test strips set.

## 2.7 Reaction kinetics analysis - optical emission spectroscopy

In order to determine the relationship between the chemical composition inside the water under treatment and plasmas parameters, the optical emission spectroscopy is employed. Figure 2.12 and Figure 2.13 illustrate two separate systems built for DBD and RF plasma. For the first one, a lens is put as close as possible to one opening of the DBD cell and used to collimate the plasma emission light into an optical fiber. The spectrometer, SpectraPro HRS-500 (Princeton Instrument), is connected to the other end of the optical fiber. The ICCD camera, PI-MAX 4 1024i (Princeton Instrument), is used to capture spectrums. A large cloth is used to cover the DBD cell and the collimated lens which reduces noise level of collected spectrums. The background correction files are collected immediately after plasmas were quenched. Settings (Intensifier, Gate Width etc.) in the LightField software are maintained the same for different pulse repetition frequencies. As for the RF plasma, we drill a hole on the water tank. The center of the hole is on the same level of the plasma's. The collimated lens is stuck inside the hole during the whole experiment and collimates the plasma emission light into the optical fiber. The spectrometer and ICCD camera are the same models as used in the DBD experiment. All light sources in our lab are closed for the purpose of reducing noise level of collected spectrums. The background correction files are collected immediately after plasmas were quenched. Settings (Intensifier, Gate Width etc.) in the LightField software are maintained the same for different system setups. For these two studies, the camera gate is always much longer than the combination of HV pulse duration and the period between two neighbor pulses, which means we acquired time-average spectra.

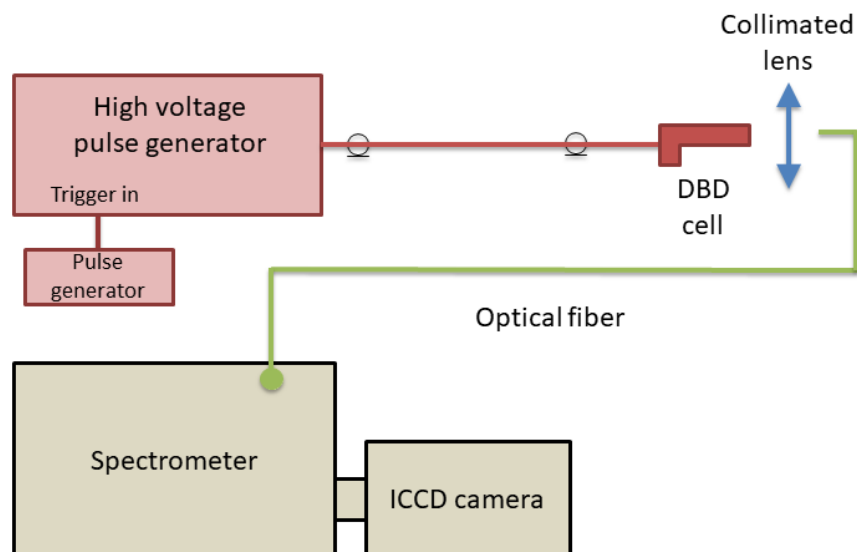


Figure 2.12: Schematic of the optical emission spectroscopy setup for DBD plasma system.

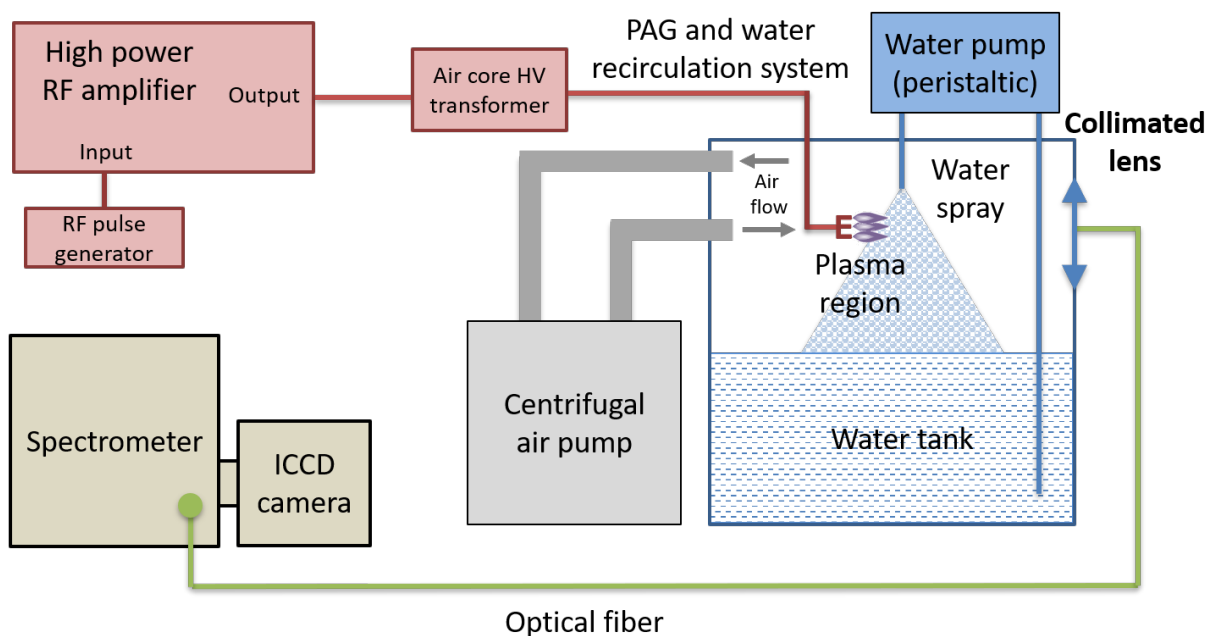


Figure 2.13: Schematic of the optical emission spectroscopy setup for RF plasma system.

To summarize, the optical emission spectroscopy is carried out with DBD pulse repetition frequencies of 30, 100, 200, 500, and 2000 Hz. As for the RF plasma, the variable is the system setup. In total, five different system setups are prepared for optical emission spectroscopy of our

RF plasma system: 1) no air flow and no water spray; 2) only fresh air in and no water spray; 3) full air circulation and no water spray; 4) full air circulation and water spray; 5) only fresh air in, water spray, and the opened lid for more air exchange.

## CHAPTER 3. CALCULATION, RESULTS, AND DISCUSSION

### 3.1 Calculation of energy consumption per one nitrate ion

Based on the data acquired from water analysis, it is possible to draw a plot between the nitrate ion concentration versus the length of treatment time. Combining with the power applied to the HV side of the plasma calculated from data collected by the oscilloscope, the energy costs per one nitrate ion for all cases are gotten and we can compare values with existing processes and literature data. The below formulas are applied:

$$\frac{\text{Energy (J)}}{\text{One ion}} = \frac{Q_{total}}{N_{total}} = \frac{P * t}{N_A * \frac{V * C}{\mu}} = \frac{P * \mu}{N_A * V * b}$$

Or

$$\frac{\text{Energy(eV)}}{\text{One ion}} = \frac{6.25 * 10^{21} * P(W) * \mu(g/mol)}{N_A * V(L) * b(mg/L/s)}$$

Where P is the electrical power applied to plasma (HV), C is the final concentration of nitrate ions,  $\mu$  is the molar mass of nitrate ion,  $N_A$  is the Avogadro constant, V is the water volume, and b is the slope in a plot of nitrate concentration versus length of treatment time.

### 3.2 Calculation of different temperatures of DBD and RF plasma

The approach adopted to determine electron temperature is to take the intensity ratio of two spectral lines. Here, we made an assumption that the population temperature of plasma is equal to the electron temperature. The intensity of the spectral line which is further assumed to be optically thin is given by:<sup>49</sup>

$$I_{ij} = \frac{hcA_{ij}g_jn}{\lambda_{ij}U(T_e)} e^{\left(\frac{E_j}{kT_e}\right)}$$

Where  $I_{ij}$  and  $\lambda_{ij}$  are the intensity and wavelength correspond to transition from  $i^{\text{th}}$  to  $j^{\text{th}}$  energy level respectively.  $h$  is the Planck's constant,  $c$  is the speed of light,  $n$  is number density of emitting species, and  $U(T_e)$  refers to partition function.  $A_{ij}$  is the transition probability between level  $i^{\text{th}}$  and  $j^{\text{th}}$ .  $k$  is the Boltzmann's constant, and  $T_e$  is the excitation temperature.  $g_j$  is the statistical weight of upper energy level and  $E_j$  is the upper energy level in eV unit. The transition probability  $A$ , statistical weight of upper energy level  $g$ , and the upper energy level  $E$  are found in Journal of Physical and Chemical Reference Data: 'Atomic Transition Probabilities of Carbon, Nitrogen, and Oxygen'.<sup>50</sup>

Next, taking the intensity ratio of two spectral lines of the same species and ionization stage, the constants will be cancelled out yielding the relationship as demonstrated below:<sup>48</sup>

$$\frac{I_1}{I_2} = \frac{A_1 g_1 \lambda_2}{A_2 g_2 \lambda_1} e^{(-\frac{E_1-E_2}{kT_e})}$$

The rotational temperatures and vibrational temperatures are inferred with spectra using the Specair software. The spectroscopy data is saved as an excel file and imported into this software. Parameters such as plasma temperatures, pressure, fractions of initial species, and radiative transitions are set manually. We use the electron temperature which is calculated in the last step as plasma temperature, atmospheric pressure, and 70% oxygen and 30% nitrogen as fractions of initial species. By changing combinations of rotational temperatures and vibrational temperatures, different synthetic spectra will be generated. The vibrational temperature strongly determines the magnitude of the intensity while the rotational temperature changes the shape of the measured band. We first go with the vibrational temperature to modify the magnitude of the intensity. Based on the closest fit (compared with the original spectrum), which can be achieved only with the change of the vibrational temperature, the rotational temperature is further modified. Lastly, the best fit is chosen, and the corresponding rotational and vibrational temperatures are recorded. We also determined the slit function of our spectrometer with 100  $\mu\text{m}$  slit opening to make the approximation more accurate. Our method is based on the assumption that the peak from the spectrum of a good laser beam should be in a shape of  $\delta$ -function. By taking the spectrum of a

laser with our spectrometer, the obtained emission line which is a product of original emission line and boarding effect should be the desired slit function. Figure 3.1 is the graph of the determined slit function.

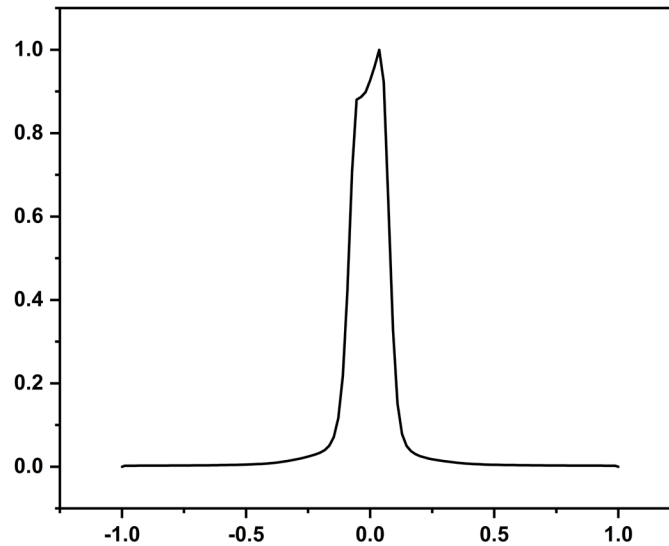


Figure 3.1: Slit function for spectrometer with 100  $\mu\text{m}$  slit setting.

### 3.3 Atmospheric pressure high temperature arc plasma

#### 3.3.1 Plasma treatment, power, and current and voltage measurements

Two different kinds of power consumption are measured as mentioned in last section: “raw” power from the powerplug which is acquired by a powermeter and HV side power calculated by voltage and current measurements with the oscilloscope (Figure 3.2).

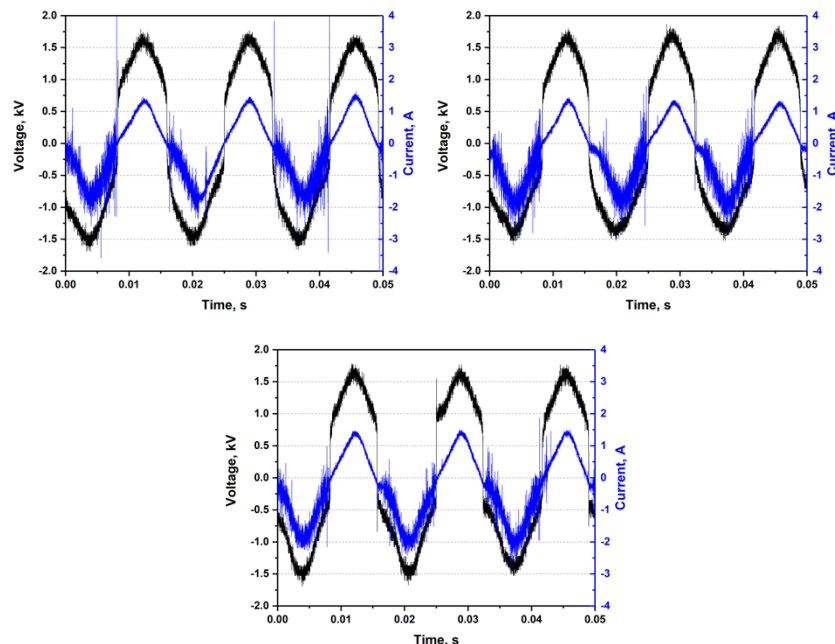


Figure 3.2: Voltage and current profiles of plasma. Different time periods are shown: (0-10) s - left, (20-30) s – bottom center, (40-50) s - right.

The peak voltage never exceeds 2 kV and the peak current is always under the calibration range which is less than 1.5 A. However, we can observe that there are some instabilities of current profile appearing on the first 10 seconds' graph (refers to the peak current exceeds 4 amperes). That is because the plasma is just ignited and not in a stable state. The directly measured ('raw') and calculated powers (HV side power) are presented on Table 3.1. According to these data, the average "raw" powerplug power is around 1300 W during the plasma treatment and HV side power is about 1050 W. The values of both power categories are without much fluctuation.

Table 3.1: “Raw” and calculated high voltage side average power.

Plasma treatment time period, s	“Raw”, powerplug power, W		HV side power, W
	Run 1	Run 2	
0-10	1370	1240	1056
10-20	1400	-	-
20-30	1400	1250	1032
30-40	1350	-	-
40-50	-	1330	1112
50-60	-	-	-
Average	1318		1067

The difference between the powerplug power and HV side power indicates that the energy conversion efficiency of our transformer is not 100%. Instead, 81% conversion efficiency is represented. We believe it is possible to design an AC-to-AC converter with 95%-98% efficiency given that an active PFC is added, and this converter is helpful if further experiments on atmospheric arc discharge would be conducted.

### 3.3.2 Water analysis

We performed plasma water treatment by igniting an arc discharge between the HV electrode and the water surface. The discharge is maintained for 5 (run 1) or 10 s (run 2) during each treatment. The overall treatment time are 40 s for the first run and 60 s for the second one. During the experiment, we noticed that the water temperature raised significantly, especially during the 10 s-lasting plasma treatment, thus we took a timeout after each treatment to wait for the beaker and water cooling back to around the room temperature. The pause time between each treatment is 100 times more than the treatment time that is 500 s for run 1 or 1000 s for run 2. That makes the atmospheric arc discharge an infeasible option for building the plasma fertilizer synthesis equipment. For both runs, 200 mL tap water is used.

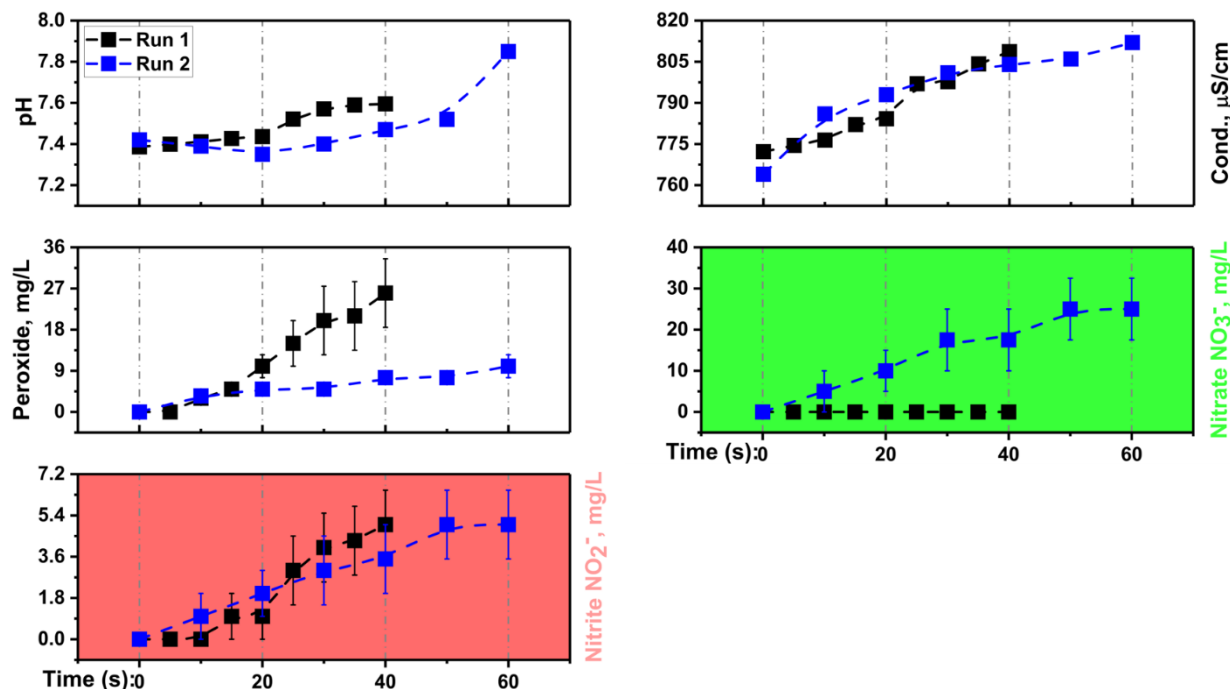


Figure 3.3: Water analysis for atmospheric pressure high temperature arc discharge: pH - up left, conductivity - up right, peroxide concentration - middle left, nitrate concentration - middle right, and nitrite concentration - bottom.

Our water analysis results are presented in Figure 3.3. In our case, energy is wasted if the final product is nitrite which means they didn't transform into nitrate at the end. Our colleague from the College of Agriculture at Purdue University (Prof. Tony J. Vyn) pointed out that nitrate ions are beneficial to plants and nitrite is profitless. As a result, we hope to produce nitrate ions as much as possible. Through this article, we marked nitrate ions concentration in green color, which means they are desirable, and nitrite in red. However, in some cases, nitrite ions are preferred and then, the production of nitrate is a waste of energy. What we can learn from these lines is that the pH value, conductivity, and nitrite concentration are comparable in both runs (not only for the value of each point but also the growth tendency). All the values increase along with time for both runs. The first disparity appears in the case of peroxide concentration. The difference between the two runs is huge. Currently, we have no exact explanation why this happens. But a reasonable guess will be that a longer heating process or higher temperature may accelerate certain chemical reactions in which peroxide is consumed, especially the oxidation process that transforms nitrite into nitrate. Since the arc discharge is temporarily regarded as an infeasible option, this problem should not be our focus at this point. Another problem is that the nitrate concentration is always

zero during the run 1. Still, our guess is based on the higher temperature run 2 can reach. There might be a plasma temperature (electron temperature, rotational temperature, vibrational temperature, or any combinations of these three) threshold only above which the nitrate ion could be produced. An indirect evidence is that the nitrite ion concentration after 40 s treatment in run 1 is about 40% higher than that in run 2. More nitrogen atoms become nitrite instead of nitrate at the end of run 1.

To further analyze this treated water, we measured all the parameters (run 2) again after 18 hours. During this period, the beaker which contains the treated water is sealed with an aluminum film. The result is summarized in Table 3.2. After 18 hours, we can observe that two ions' concentrations somewhat decay. One exemption is the concentration of nitrate ion. The value slightly increases after 18 hours. The reason is that some nitrite ions are oxidized by peroxide or residual oxygen inside the beaker and transform into nitrate ions eventually. However, this reaction only happens when the nitrite concentration is low (several milligrams per liter). If the nitrite concentration is very high, then, it will not transform into nitrate even with the appearance of a large amount of oxidizer. Also, the pH value further goes up. Combined with the above-mentioned increase of pH value, it is possible that some alkaline substances are produced at the start of plasma treatment (at least first 40 seconds) along with the peroxide, nitrite, and nitrate. The production rate of alkaline substances could be faster than that of acids.

Table 3.2: Water parameters after 18-hour standing time.

Time	p.H.	Conductivity ( $\mu\text{S}/\text{cm}$ )	Peroxide ( $\text{mg}/\text{L}$ )	Nitrite ( $\text{mg}/\text{L}$ )	Nitrate ( $\text{mg}/\text{L}$ )
Stands for 18 hours	8.033	820.7	15	2	27

Applying the formulas described in section 3.1, the energy cost per one ion could be calculated. The results are summarized in the Table 3.3. It is not surprising that the energy consumption is huge since plenty of it is transformed into the form of heat. This accounts for the rapidly raising temperature of water inside the beaker.

Table 3.3: Energy costs per one nitrate/nitrite ion for high temperature plasma arc.

Ion	Molar mass, g/mol	Slope b, mg/L/s	Energy per one ion, eV	
			"Raw" powerplug, 1318 W	HV side, 1067 W
Nitrate ( $\text{NO}_3^-$ )	62	0.44	$\approx 9600$	$\approx 7800$
Nitrite ( $\text{NO}_2^-$ )	46	0.087	$\approx 36000$	$\approx 29000$

### 3.4 Atmospheric pressure DC positive corona discharge

#### 3.4.1 Plasma treatment, power, and current and voltage measurements

Both corona configurations (pin to water or pin to metal mesh) share the same voltage and current profiles. Firstly, let us consider the plasma current. It has two components: several sharp peaks with a duration of about 0.14 ms and a quasi-DC component with very slow decay. This decay can be observed more clearly on the right graph of Figure 3.4. In the following sections, we will consider the quasi-DC component as a constant current without loss of accuracy.

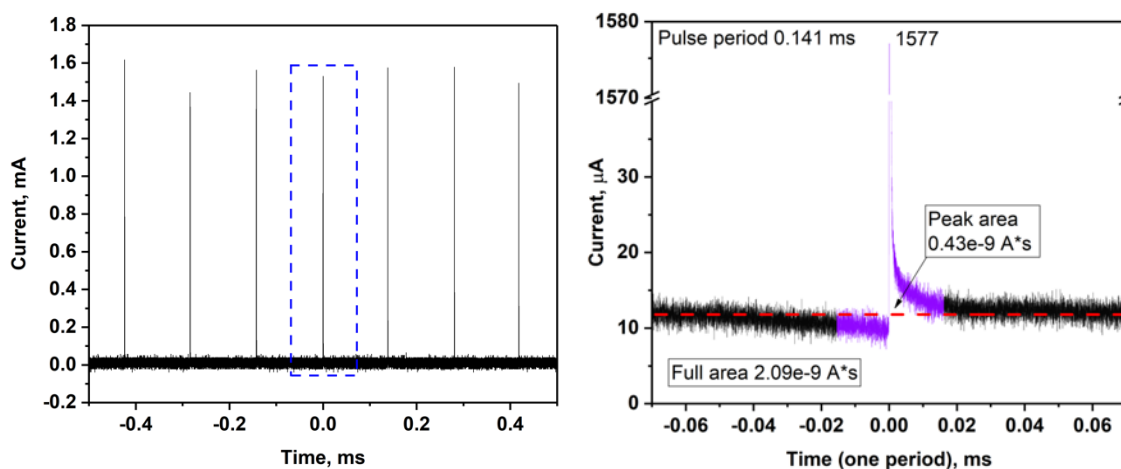


Figure 3.4: Current through a corona discharge. Overview on the left and one pulse zoom on the right.

As for the applied voltage, it is constant 8 kV with less than 40 V fluctuations. Neither voltage nor current waveforms change during the plasma treatment. Furthermore, overall plasma electrical power consumption (or, in other words, HV side power) is calculated. Like the plasma current, it

is divided into two components - 24 mW for the pulse and 96 mW for the quasi-DC component. In total, the power is 120 mW. It is important to notice that the power plug power consumption is 19 W during the test. Thus, we can conclude that the major part of power consumption goes into heat and other dissipation sources (like a working fan etc.) inside the DC HV power supply. Taking into account the modern power supply design achievements, we think it is possible to develop a special HV DC power supply for corona discharge with around 90% power efficiency.

### 3.4.2 Water analysis

We performed plasma water treatment by igniting a corona discharge between the HV electrode and the water surface for pin to water run (run 1) and between HV electrode and metal mesh for pin to mesh run (run 2). The discharge is maintained for 600 s during each treatment for both runs. However, we took three more special points for run 2 at overall treatment time of 3600, 4800, and 6000 s which serves as the purpose to check whether longer treatment time will have special effects on water properties. The overall treatment time are 3000 s for the first run and 6000 s for the second one. For both runs, 10 mL distilled water is used.

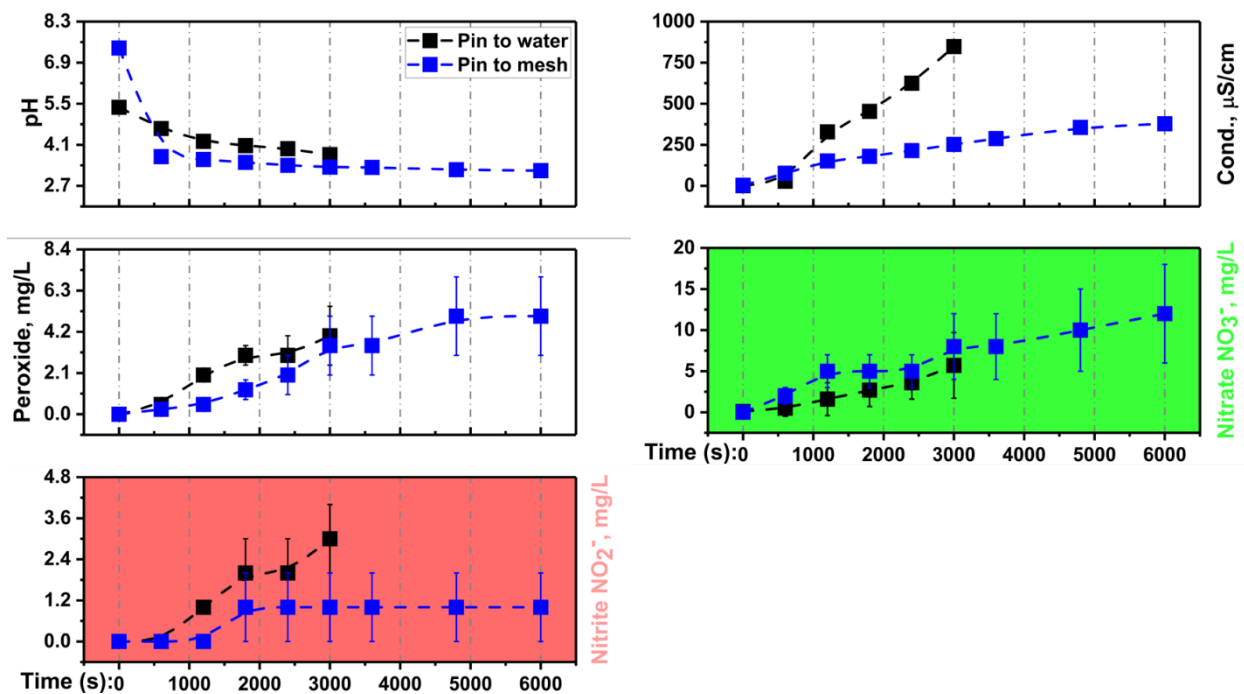


Figure 3.5: Water analysis for atmospheric pressure DC positive corona discharge: pH - up left, conductivity - up right, peroxide concentration - middle left, nitrate concentration - middle right, and nitrite concentration - bottom.

Our water analysis results are presented in Figure 3.5. What we can learn from these lines is that the pH value, peroxide concentration, and nitrate concentration are comparable in both runs (not only for the value of each point but also the growth tendency). All these values increase along with time for both runs. Longer treatment time for run 2 has no additional effect on these water properties. For the pin to mesh configuration, the pH value and the peroxide concentration are lower. However, the nitrate concentration is slightly higher. The first disparity appears in the case of conductivity. The difference between the two runs is huge. At the point of 3000 s total treatment time, the conductivity of water under pin to water configuration is almost 4 times higher than that under pin to mesh configuration. It seems that more ions, besides the nitrate, nitrite, and peroxide, are produced under the pin to water configuration. Another point that should be paid attention to is the nitrite concentration. For run 2, after 2000 s, the nitrite concentration stays the same. It is also true for the peroxide concentration. But it happens after 5000 s overall treatment time. These facts demonstrate that reaction kinetics for discharges under the same current and voltage profiles but with various configurations are totally different.

Table 3.4: Energy costs per ion for atmospheric pressure positive DC corona discharge.

Ion	Molar mass, g/mol	Slope b, mg/L/s	Energy per one ion, eV	
			"Raw" powerplug, 19 W	HV side, 120 mW
Nitrate (NO <sub>3</sub> <sup>-</sup> )	62	0.00185	≈6.6E5	≈4100
Peroxide (H <sub>2</sub> O <sub>2</sub> )	34	0.00117	≈5.7E5	≈3600

Applying the formulas described in section 3.1, the energy cost per one ion could be calculated. The results are summarized in the Table 3.4. It is not surprising that the energy consumption based on raw power is huge since plenty of it is transformed into the form of heat which is dissipated inside the DC HV power supply as mentioned before. The real energy consumption per one nitrate ion for atmospheric pressure DC positive corona discharge is a half lower than the atmospheric pressure arc discharge.

### 3.5 DC voltage driven cold plasma torch operating with helium

#### 3.5.1 Plasma treatment, power, and current and voltage measurements

According to our observations, there are at least three different discharge regimes in this DC voltage driven cold plasma torch. When the applied voltage is around 5kV (The value may vary from 4.98 kV to 5.01 kV. The number changes several times even in an hour. One possible assumption for this phenomenon is that the plasma torch is very sensitive to the surrounding's humidity), the current curve has two components: a sharp peak and a horizontal line which is followed (similar to atmospheric pressure DC positive corona discharge). With the increase of the voltage, the plasma torch becomes unstable accompanied with unremitting and random sparks. In terms of the current, there is no fixed frequency of the peak occurrence. Finally, only DC component of the current remains (compared with the first regime). An extremely dim plasma is found at the outlet of the plasma torch.

For our project, we utilized the plasma generated in the first regime. As usual, let us consider the plasma current first. It has two components: sharp peaks with the period of about 1.25 ms and a permanent DC current with a value of 1  $\mu\text{A}$ . These pulses and the permanent DC current can be illustrated more clearly with the help of the right and bottom graphs of Figure 3.6.

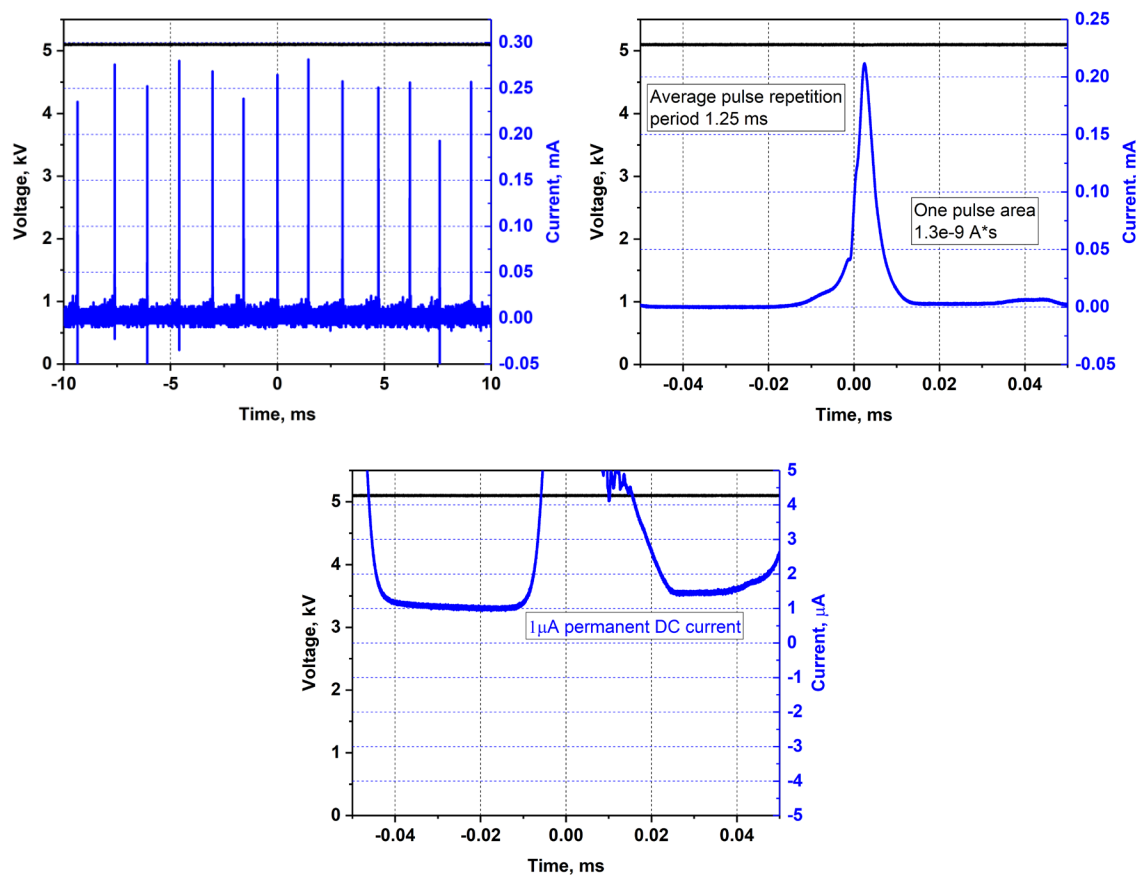


Figure 3.6: Current through a Helium plasma torch. Overview on the top left and one pulse zoom on the top right. The bottom graph shows the permanent DC current component.

The applied voltage was constant 5.1 kV with less than 20 V fluctuations. Neither voltage nor current waveforms changed during the plasma treatment. Further, overall plasma electrical power consumption (or, in other words, HV side power) was calculated and like the plasma current, it is divided into two components - 5.3 mW for the pulse and 5.1 mW for the permanent ones. The total power for the plasma is 10.4 mW. It is the same as what we observed in atmospheric pressure DC positive corona discharge that the major part of power consumption goes into heat and other dissipation sources inside the DC HV power supply. The powerplug power consumption is around

10 W. The expected maximum power efficiency could reach 90% with specially designed DC HV power supply.

### 3.5.2 Water analysis

We performed plasma treatment by using the described plasma torch. The overall treatment time is 3600 s. Water properties are measured each 600 s. Distilled water was used.

Through our experiment, there is no sign of peroxide and nitrite production in the treated water. The pH value, conductivity, and the concentration of nitrate are described in the Figure 3.7. There is a strange point in the water conductivity graph which should be paid attention to. From 600 s to 1200 s, the conductivity increases sharply. Before this 10-minute treatment, the experiment had been stopped for an hour and the treated water was covered with a clean lid. We do observe the same increase of conductivity in the later DBD plasma treatment experiment, if standing time is applied between each run. Currently, no specific explanation has been figured out. One possible guess is that more ions are available to move freely after the applied standing time. Initially, these produced ions are bonded with molecules, such as water. After the standing time, they manage to get away from the control of molecule and become free ions which contribute to the increase of conductivity. The maximum nitrate concentration is 3.5 mg/L.

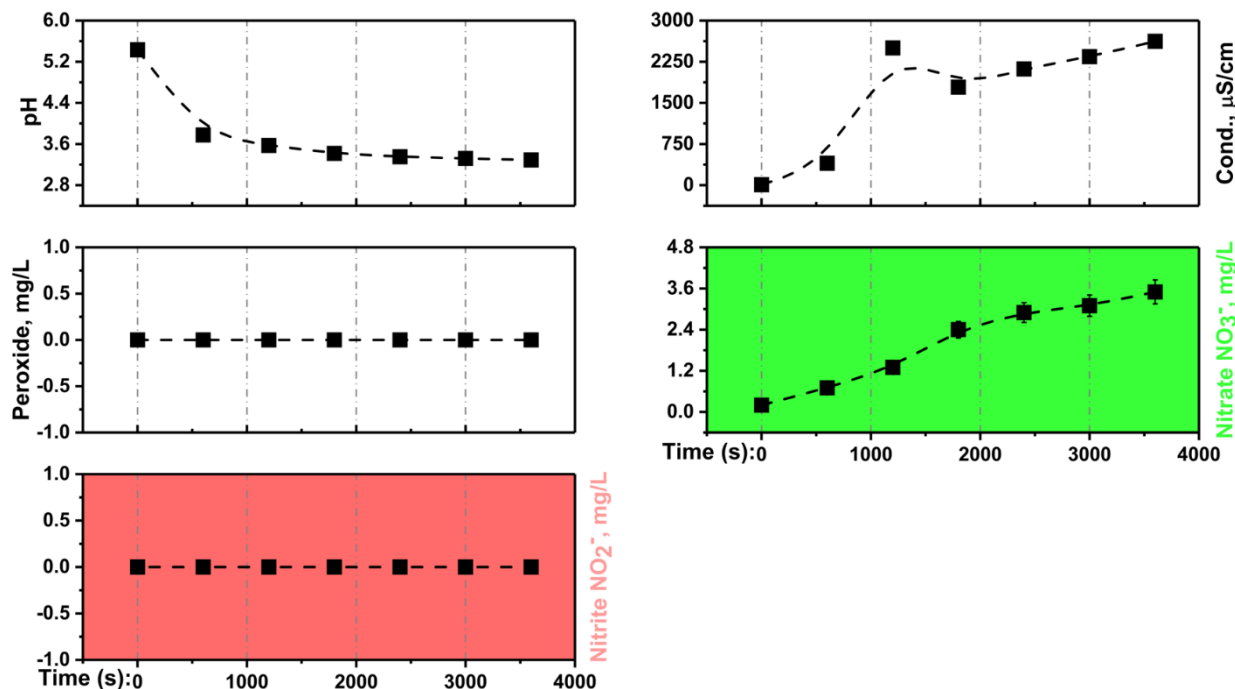


Figure 3.7: Water analysis for DC voltage driven cold plasma torch: pH - up left, conductivity - up right, peroxide concentration - middle left, nitrate concentration - middle right, and nitrite concentration - bottom.

Applying the formulas described in section 3.1, the energy cost per one nitrate ion could be calculated. The results are summarized in the Table 3.5. Again, it is not surprising that the energy consumption based on raw power is huge since plenty of it is transformed into the form of heat which is dissipated inside the DC HV power supply. The real energy consumption per one nitrate ion for this cold plasma torch operating with helium is one order of magnitude lower than those for the previous two plasma sources. The main problem of this discharge is the low productivity. Only 3.5 mg/L nitrate ions are accumulated in an hour. It is a time-wasting process.

Table 3.5: Energy costs per one nitrogen ion in Helium plasma torch treatment process.

Ion	Molar mass, g/mol	Slope b, mg/L/s	Energy per one ion, eV	
			"Raw" powerplug, 10 W	HV side, 10.4 mW
Nitrate ( $\text{NO}_3^-$ )	62	0.00097	$\approx 6.6\text{E}5$	$\approx 690$

### 3.6 Atmospheric pressure dielectric barrier discharge

#### 3.6.1 Plasma treatment, power, and current and voltage measurements

The pulser output voltage was set to be 5 kV, and because our plasma cell's impedance is much higher than the cable's, the actual voltage amplitude on the plasma cell is doubled, almost 10 kV, and the maximum pulse current is 40 A. After being reflected from the cell, the HV pulse travelled back along the cable and then reflected at the other end of it, where the pulser was connected. This process happened many times (Figure 3.8, left) and the pulse attenuated when it moved forward and backward through the cable. As a result, the magnitude of both voltage and current damped with the increase of time. We further multiplied the time-resolved voltage and current together to get the real-time power. Then, by integrating of this power with time, the energy per pulse was gotten (Figure 3.8, right). The calculated energy per pulse is 2.47 mJ for 500 Hz PRF.

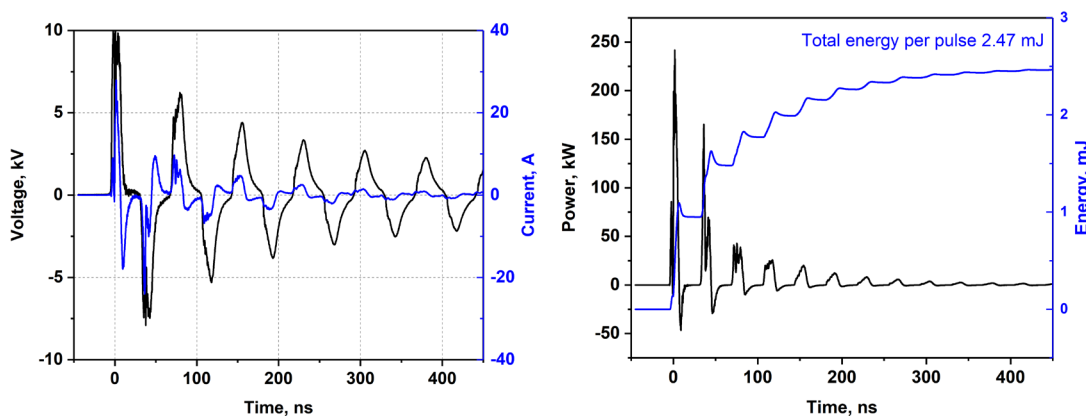


Figure 3.8: Voltage and current profiles (left) and energy per pulse (right).

#### 3.6.2 Water analysis

Figure 3.9 summarizes the change of all five water parameters that are focused throughout this research - pH value, water conductivity, peroxide concentration, nitrite concentration, and nitrate concentration with the duration of 500 Hz-frequency DBD plasma treatment in 500 mL water. It seems that the change of nitrate concentration is closely related to the change of water conductivity

because: 1. The nitrate ion dominates the water solution. The concentration of it is far greater than that of the peroxide and nitrite. As a result, the water concentration is largely influenced by this ion; 2. Fittings for the points on the diagrams for water conductivity and nitrate concentration are similar which means the growth trends for these two are the same. Another thing that should be paid attention to is the nitrite concentration, which is zero. This situation is desirable since the main purpose of this research is to increase the energy efficiency for producing nitrate in water. The pH value decreases after the first 500 seconds treatment and then returns to its initial value after 1800 seconds treatment. The conductivity of water increases monotonically and approximately linearly during the whole treatment. As mentioned previously, the nitrate concentration grows monotonically and thus, a large amount of hydrogen ions will be produced simultaneously which will result in a continuous reduction of pH value. It is reasonable to assume that something alkaline is produced after 1000 seconds. Although the concentration of peroxide is relatively small, the appearance of it proves the oxidizability of the water after plasma treatment. This feature is important since it can assure that nitrogen atoms can exist in the form of nitrate ions for a longer time.

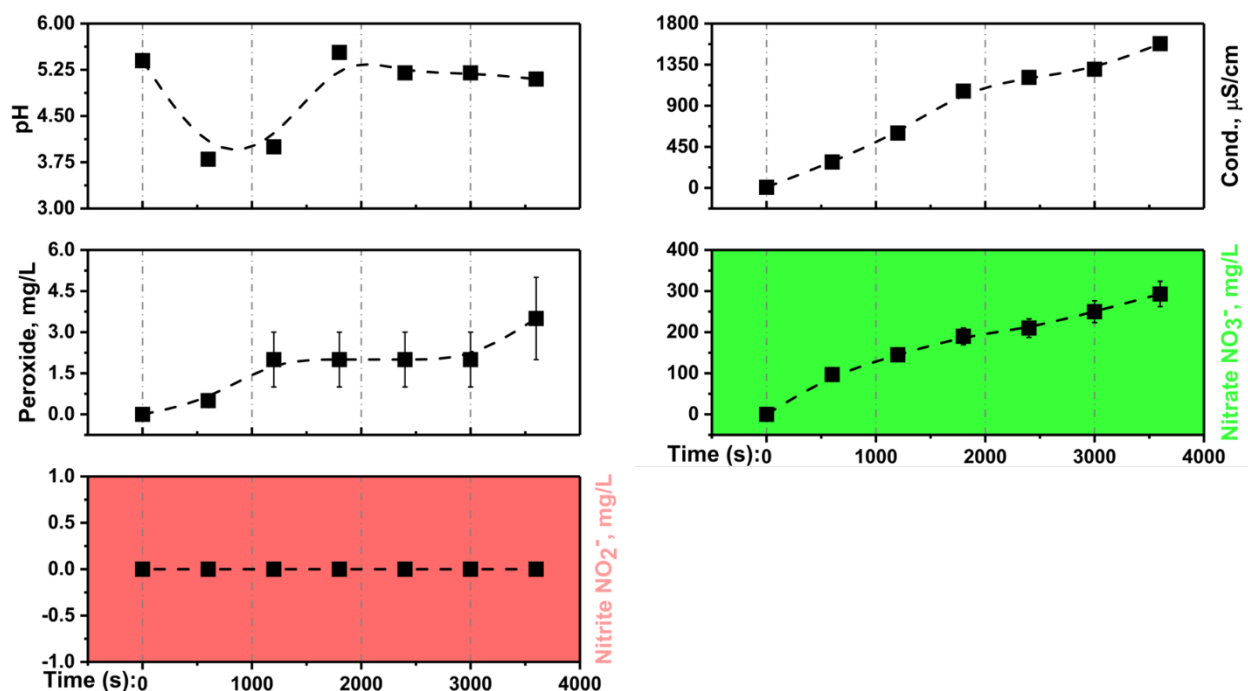
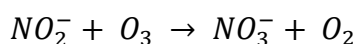


Figure 3.9: Water analysis for 500Hz-frequency DBD treatment in 500 mL water: pH - up left, conductivity - up right, peroxide concentration - middle left, nitrate concentration - middle right, and nitrite concentration - bottom.

Figure 3.10 presents the comparison between water properties after 500 and 2000 Hz PRF DBD treatment in 500 mL water. More nitrate ions are produced at the end of the 2000 Hz-frequency DBD treatment: around 500 mg/L after the 2000 Hz-frequency DBD plasma treatment compared to less than 300 mg/L in 500 Hz case. However, a large amount of nitrite ions is produced as a by-product. It is not surprising to observe that the peroxide concentration decreases a little bit since part of it may react with those nitrite ions and transform into nitrate ions immediately. The following reaction is the explanation:



It has been discussed that the appearance of nitrite ions will lower down the energy efficiency which means that the energy required to produce one nitrate ion increases in the 2000 Hz case. The pH value changes with the same pattern as observed in 500 Hz case. The conductivity of water is almost two times higher due to the increase of nitrate and nitrite concentration.

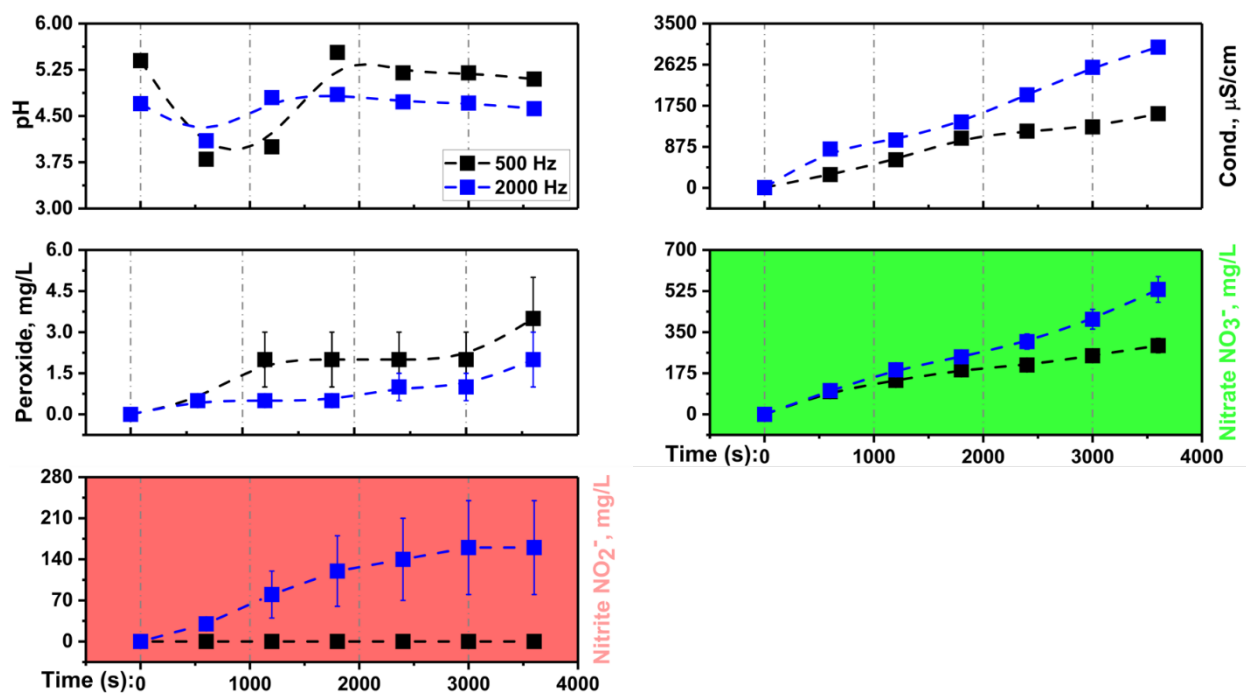


Figure 3.10: Comparison between 500 Hz- and 2000 Hz-frequency DBD treatment in 500 mL water: pH - up left, conductivity - up right, peroxide concentration - middle left, nitrate concentration - middle right, and nitrite concentration - bottom.

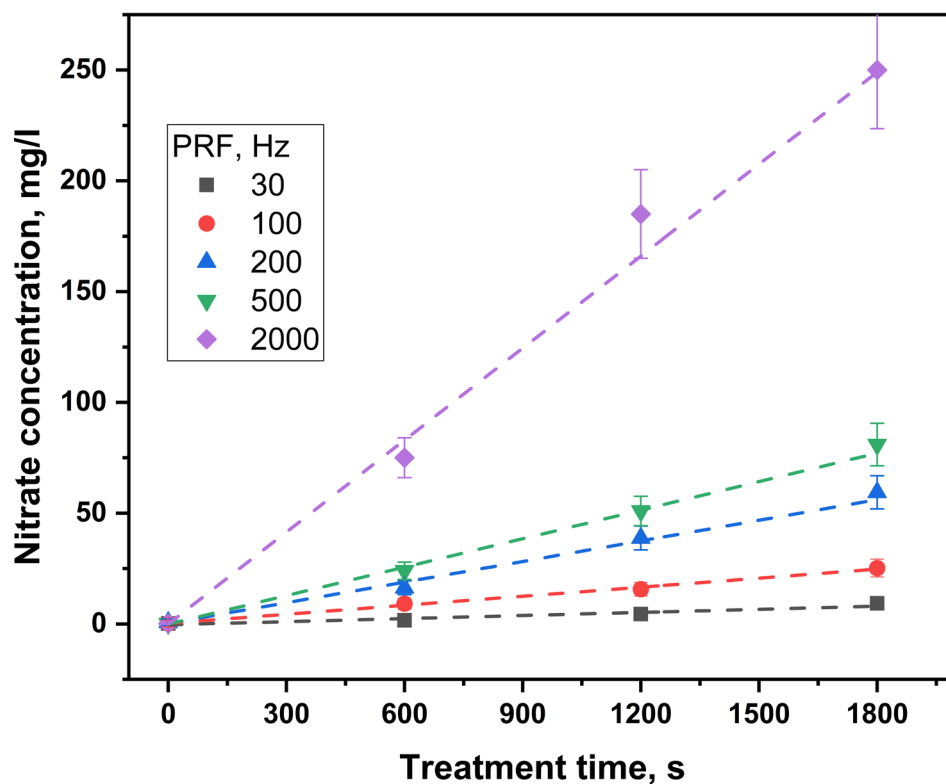


Figure 3.11: Nitrite concentration for different DBD pulse repetition frequencies in 10 mL water tank.

Based on the above data, it is possible to calculate the energy cost per one nitrate ion for all cases with the formulas described in section 3.1. The calculation results for 30, 100, 200, 500 and 2000 Hz with two water volumes are presented for comparison. Nitrate concentration, as well as the excited species production rate, grow with the increase of PRF. However, calculated energy cost per one nitrate ion in the water also increases with PRF. At low PRF, the energy cost reaches 500 eV/ion with large water volume – 500 mL. It appears that the 200-500 Hz pulse repetition frequency is a good “middle ground” between high nitrate production rate and acceptable energy efficiency. 500 mL water volume, in comparison with 10 ml one, has several benefits. First, air bubbles travel a longer distance in the water and spend more time in contact with it. Second, larger water volume helps to keep the concentration of reaction products low much longer, which suppresses reverse reactions. Energy costs per one nitrate ion are summarized in Figure 3.12.

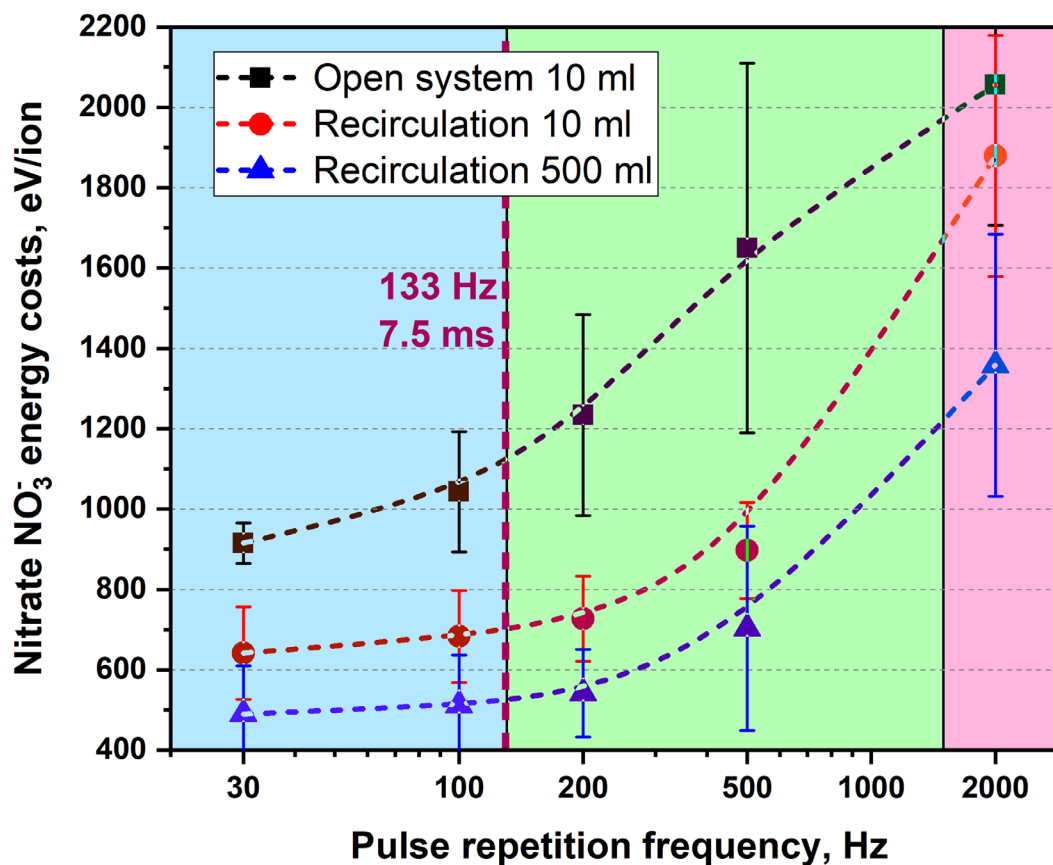


Figure 3.12: Nitrate energy costs versus pulse repetition frequency in three systems.

### 3.6.3 Optical emission spectroscopy

Our goal is to reduce the energy cost per one nitrate ion produced during the DBD plasma water treatment as low as possible. It is important to understand the mechanism behind which determines the energy consumption during the production of nitrate ions. In other word, we want to understand why the energy cost at 30-Hz pulse repetition frequency is the lowest. As a result, optical emission spectroscopy is employed to study the reaction kinetics. Figure 3.13 shows emission lines for DBD plasma with different pulse repetition frequencies: 30, 100, 200, 500, and up to 2000 Hz. All emission lines are from  $N_2^+$  first negative and  $N_2$  second positive systems. Table 3.6 summarizes the relationship between emission lines and two nitrogen systems.

Table 3.6: Emission lines' wavelength and their corresponding systems.

System	Emission line's wavelength (nm)
N <sub>2</sub> first negative system	391.527, 427.813
N <sub>2</sub> second positive system	311.658, 313.593, 315.928, 333.928, 337.173, 349.992, 353.627, 357.654, 370.991, 375.479, 380.503, 399.767, 405.891, 420.039, 426.872, 434.423

No new emission line appear along with the increase of DBD pulse repetition frequency. However, a large amount of nitrite (150 mg/L) is produced if the pulse repetition frequency is set to 2000 Hz. The reason accounted for this contradiction is that the intensity of nitrogen second positive system emission lines is so strong that they might cover the new emission lines produced by nitrite ions. Second order diffraction lines are filtered out and Figure 3.14 shows the details of them. All peaks whose wavelength is greater than 590 nm have been determined to be second order diffraction lines.

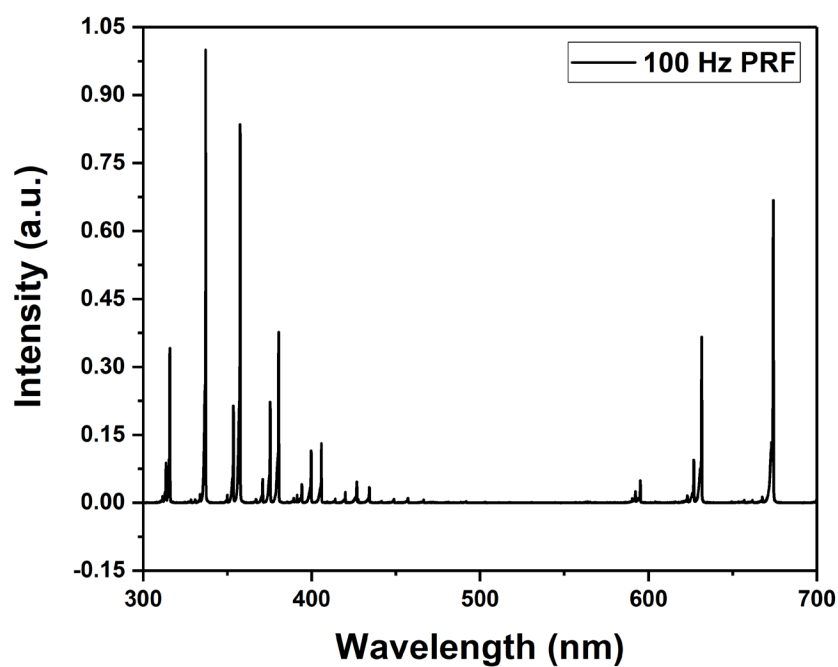
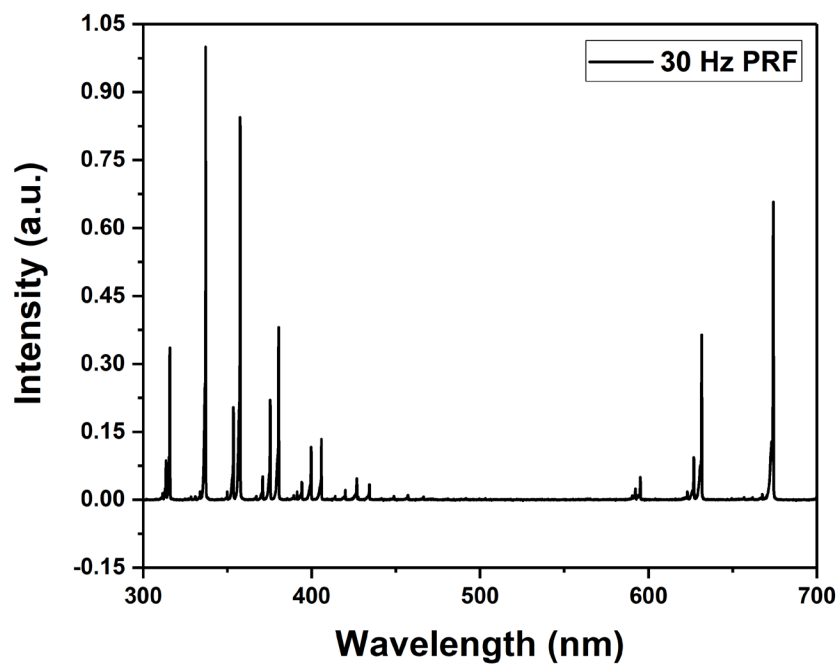


Figure 3.13: Spectrums for DBD with different pulse repetition frequencies (from top to bottom: 30 Hz, 100 Hz, 200 Hz, 500 Hz, and 2000 Hz).

Figure 3.13: continued.

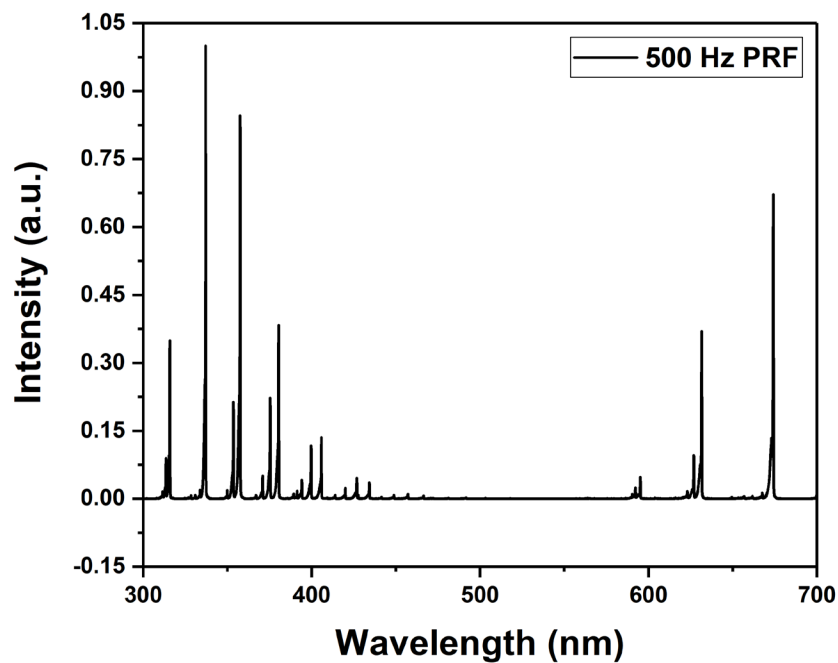
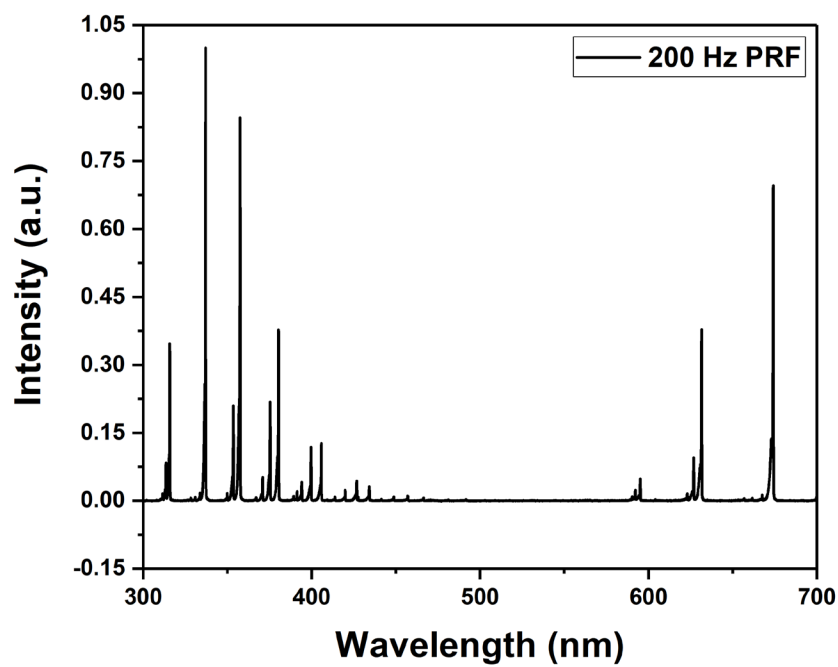
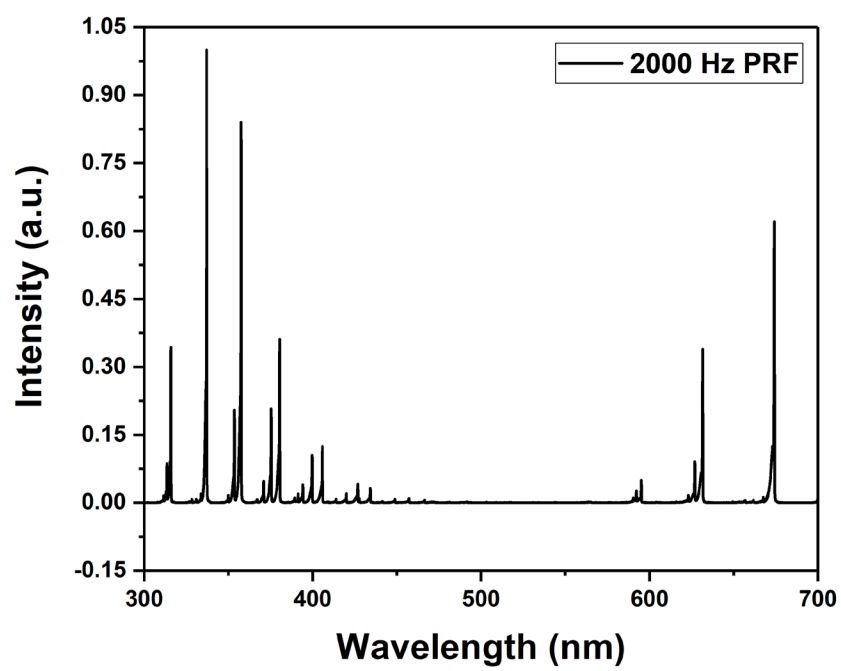


Figure 3.13: continued.



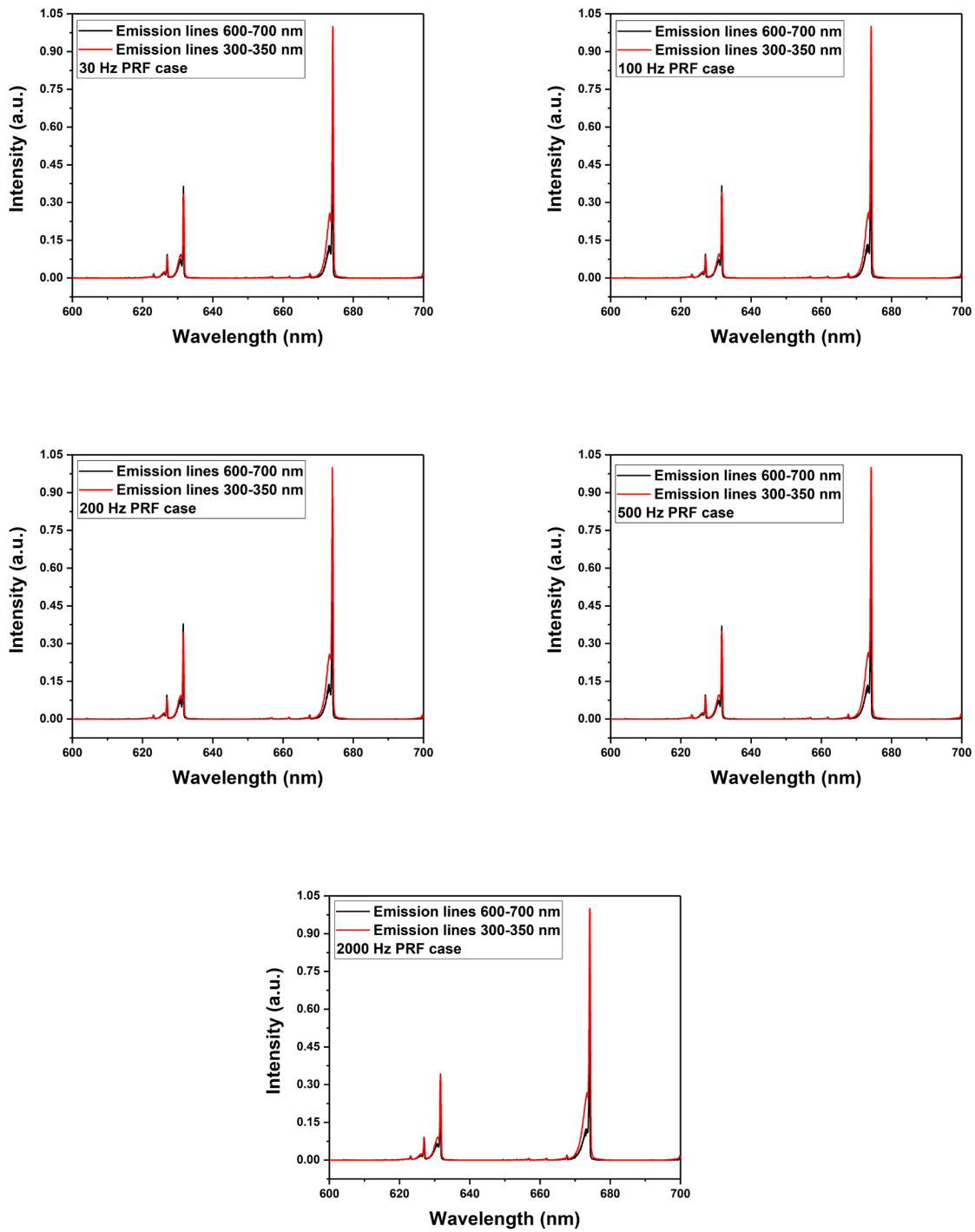


Figure 3.14: Second order diffraction test for DBD with different pulse repetition frequencies (from top to bottom and from left to right: 30 Hz, 100 Hz, 200 Hz, 500 Hz, and 2000 Hz).

### 3.6.4 DBD temperatures calculation and possible reaction kinetics

Table 3.7 summarizes the relations between different PRF and three temperatures mentioned above. From the table, the first thing that should be paid attention to is that the electron temperature and the vibrational temperature almost stays the same at different PRFs. However, at higher PRF, the rotational temperature is also higher. Combining with the fact discovered while conducting water analysis that nitrite is produced when the PRF is increased to 2000 Hz, it is reasonable to purpose that the production of nitrite in this DBD system is closely related to the rotational temperature.

Table 3.7: Three temperatures under different PRFs.

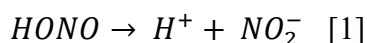
PRF, Hz	Electron temperature, eV	Rotational temperature, K	Vibrational temperature, K
30	3.9	350	2950
100	3.8	400	3150
200	3.7	410	2900
500	3.6	430	3100
2000	3.7	500	3000

Our hypothesis is summarized in Table 3.8.

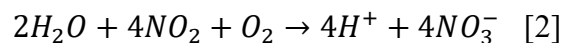
Table 3.8: Reaction kinetics at different pulse repetition frequencies.

PRF that is less than the critical PRF, low rotational temperature	PRF that is equal to or higher than the critical PRF, high rotational temperature (around 500 K)
<p style="text-align: center;">Gas phase</p> <p style="text-align: center;"><i>Humid air</i> <math>\xrightarrow{\text{Plasma}}</math> <math>NO_2, O_3, H_2O_2</math></p>	<p style="text-align: center;">Gas phase</p> <p style="text-align: center;"><i>Humid air</i> <math>\xrightarrow{\text{Plasma}}</math> <math>NO_2, \mathbf{HONO}, O_3, H_2O_2</math></p>
<p style="text-align: center;">Liquid phase</p> <p style="text-align: center;"><math>H_2O + 3NO_2 \rightarrow 2H^+ + 2NO_3^- + NO</math></p> <p style="text-align: center;"><math>2H_2O + 4NO_2 + O_2 \rightarrow 4H^+ + 4NO_3^-</math></p>	<p style="text-align: center;">Liquid phase - same reactions with <math>NO_3</math></p> <p style="text-align: center;">Plus</p> <p style="text-align: center;"><math>HONO(gas) \rightarrow HNO_2(liq) \rightarrow H^+ + NO_2^-</math></p> <p style="text-align: center;"><b>NO doesn't react with water</b></p>

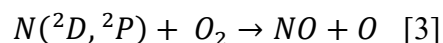
It is important to notice that the reaction below is the major way to produce nitrite ions in the water:

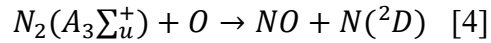


Nitrogen dioxide, on the contrary, will produce nitrate ions when dissolving into water and under the condition of abundant oxygen:

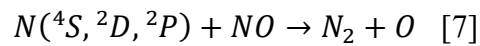
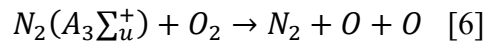
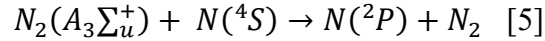


When the rotational temperature increases, we observed the concomitant increase of energy consumption to produce one nitrate ion. However, the concentration of nitrite ions is nearly zero up to the pulse repetition frequency of 500 Hz. Below 500 Hz PRF, the reason accounted for the increased energy consumption may be the suppression of the nitric oxide molecules. Two major reactions to produce NO are:





These following three reactions will consume raw materials which will be used for the generation of NO:



As the rotational temperature increases, the reaction rates of [5], [6], and [7] will also increase. As a result, reaction [3] and [4] will be suppressed which will lead to less nitrate ions produced according to reaction [2]. That is an explanation for the increased energy consumption at higher PRF up to 500 Hz. At 2000 Hz, HONO is produced and that is a more direct way to show why energy consumption increases. One possible explanation for this phenomenon was put forward. In the future, we plan to employ residual gas analyzer (RGA) to do deeper study in the reaction kinetics of DBD under different PRFs and the obtained results should help verify this aforementioned possible explanation.

### 3.7 Atmospheric pressure radio frequency plasma

#### 3.7.1 Plasma treatment, power, and current and voltage measurements

After being amplified, the output voltage on the high voltage side of the air core resonance transformer exceeds the measurable value. Additionally, doing measurements on the high voltage side will change the transformer's resonance frequency. This resonance frequency is 424 kHz. Based on these two reasons, the voltage and current profiles are taken from the low voltage side. The maximum voltage on LV side of the plasma source is almost 350 V and the maximum pulse current is 2.5 A. The magnitude of both voltage and current damp with the increase of time (Figure

3.15, left). We further multiplied the time-resolved voltage and current together to get the real-time power. Then, by integrating of this power with time, the energy per pulse was gotten (Figure 3.15, right). The power transferring efficiency for this Tesla coil at its resonance frequency is 87%. The calculated energy per pulse is 2.18 mJ on the HV side of plasma, or 27 W average plasma power.

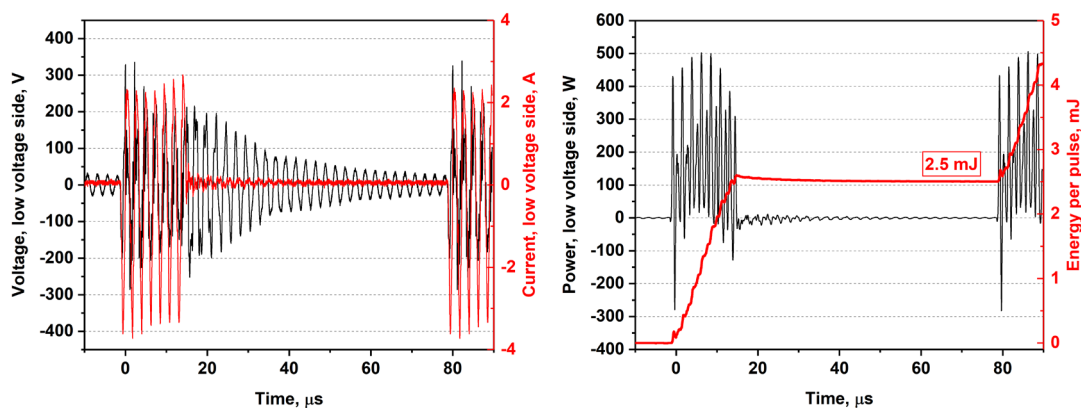


Figure 3.15: Voltage and current profiles (left) and energy per pulse (right) on LV side of the plasma.

### 3.7.2 Water analysis

Figure 3.16 summarizes the change of all five water parameters that are focused throughout this research - pH value, water conductivity, peroxide concentration, nitrite concentration, and nitrate concentration within the duration of RF plasma treatment. The volume of water is 4 liters. Same as the treatment performed with dielectric barrier discharges, the change of nitrate concentration is closely related to the change of water conductivity because: 1. The nitrate ion dominates the water solution. The concentration of it is even farther greater than that of the peroxide and nitrite compared with the DBD case (almost two orders of magnitude); 2. Fittings for the points on the diagrams for water conductivity and nitrate concentration are exactly the same which means the growth trends for these two are similar. The nitrite ion concentration is around 15 mg/L and it is almost negligible compared to the nitrate concentration. We can safely assume that no energy is wasted on producing nitrite ions (as mentioned in section 3.3.2, the energy consumed to produce nitrite ions, given that they have not been oxidized into nitrate ions eventually, is regarded as a waste only in our project). Unlike the DBD case, the pH value decreases monotonically, and the

peroxide concentration is zero for all the time. With the slope  $b$  calculated from the nitrate concentration graph and formulas described in section 3.1, the energy consumption per one nitrate ion produced with RF plasma is 390 eV.

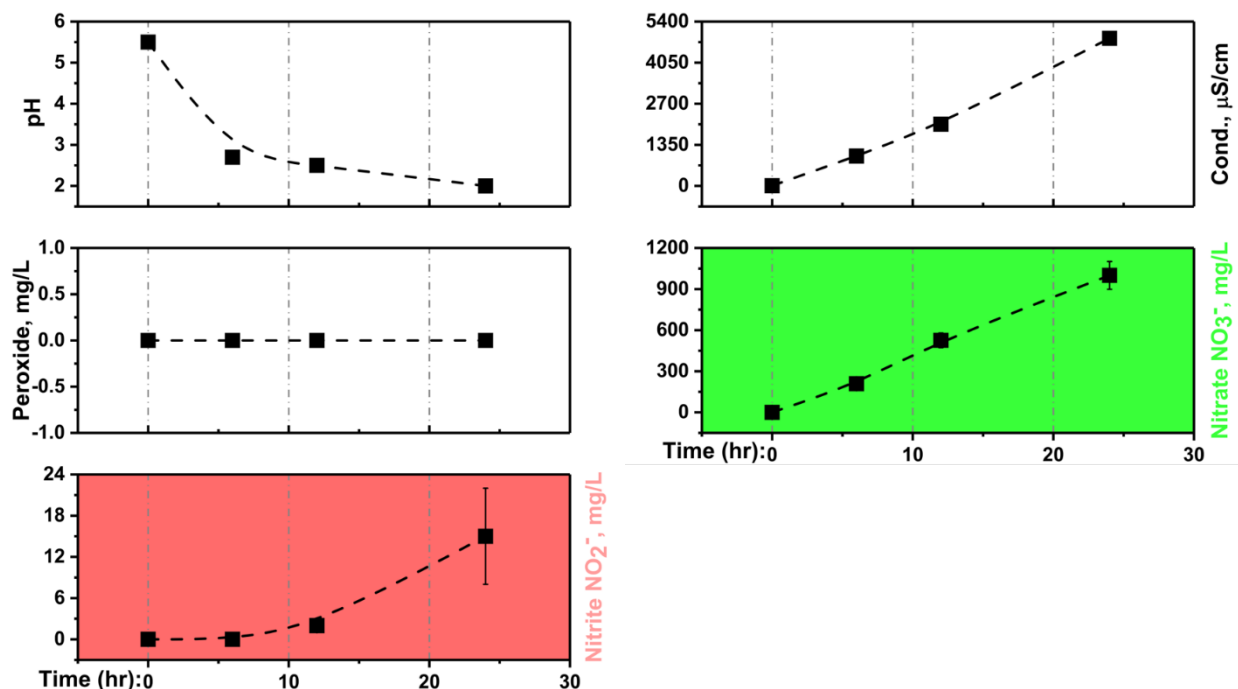


Figure 3.16: Water analysis for RF plasma treatment with 4 L water: pH - up left, conductivity - up right, peroxide concentration - middle left, nitrate concentration - middle right, and nitrite concentration - bottom.

### 3.7.3 Optical emission spectroscopy

Optical emission spectroscopy is carried out with the RF plasma under five different system setups: 1) no air flow and no water spray (the fully closed chamber); 2) only fresh air in and no water spray (inhale fresh and cool air from outside environment); 3) full air circulation and no water spray (the fully closed chamber but with air movements); 4) full air circulation and water spray (use water to cool down the air inside the chamber); 5) only fresh air in, water spray, and the opened lid for more air exchange. No new peak, except those described in Table 3.6, appears on the spectrums of all five tested cases. It is not strange since the nitrite concentration is much lower than the nitrate concentration this time. We cannot draw a single conclusion only based on these spectrums. All the five spectrums look similar to each other. Figure 3.17 presents the spectrums

for RF plasma under five experiment setups. One point to be noticed is that no second order diffraction lines are displayed on all spectrums. They are automatically filtered out by the spectrometer. Different from the spectrums for DBD, under no water spray condition, the peaks with wavelengths falling in the range from 300 to 320 nm are more intensive and the peaks with wavelengths greater than 350 nm are less intensive which proves that the reaction kinetics for atmospheric pressure DBD and RF plasma are different. However, with water spray, the intensity of lines with wavelength greater than 350 nm increases. We can conclude that water molecules do join the reactions happening within the plasma region. One last thing to be pointed out is that the noise level of the spectrums for RF plasma with water spray is slightly higher than that without the water spray. We inserted the collimated lens directly into the water tank. Water drops injected from water spray heads and water vapor produced due to high temperature inside the chamber will accumulate on the lens outer surface.

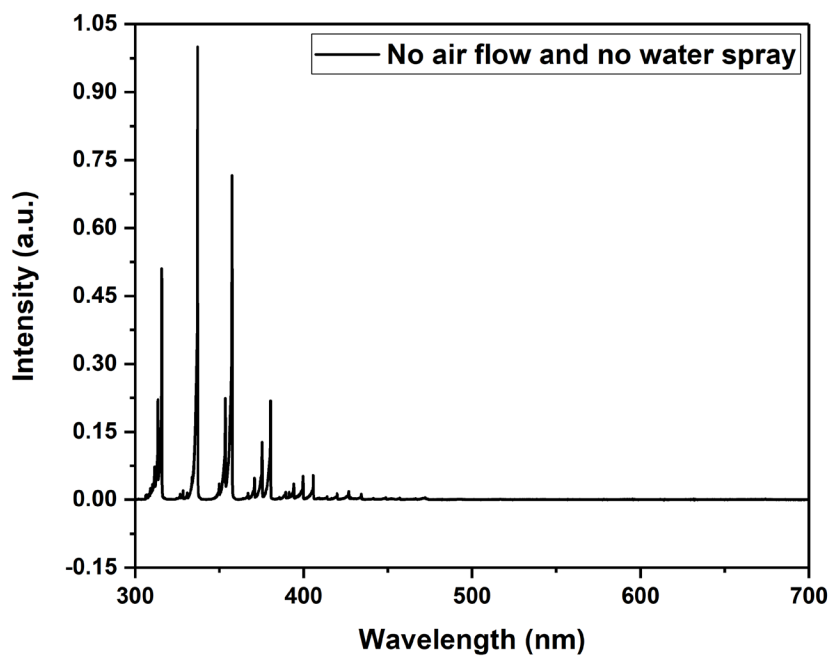


Figure 3.17: Spectrums for RF plasma with different experiment setups (from top to bottom and from left to right: no air flow and no water spray, only fresh air in and no water spray, full air circulation and no water spray, full air circulation and water spray, and only fresh air in, water spray, and opened lid).

Figure 3.17: continued.

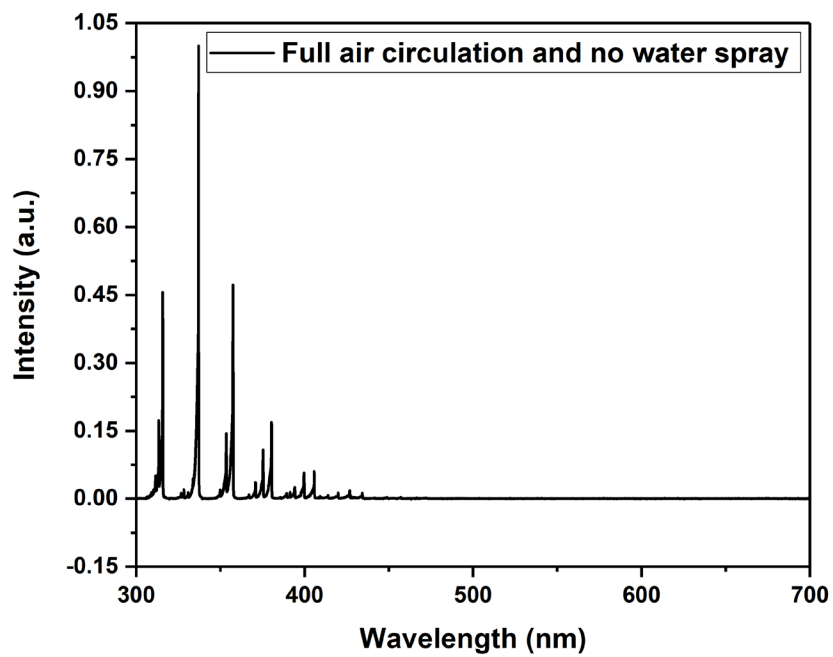
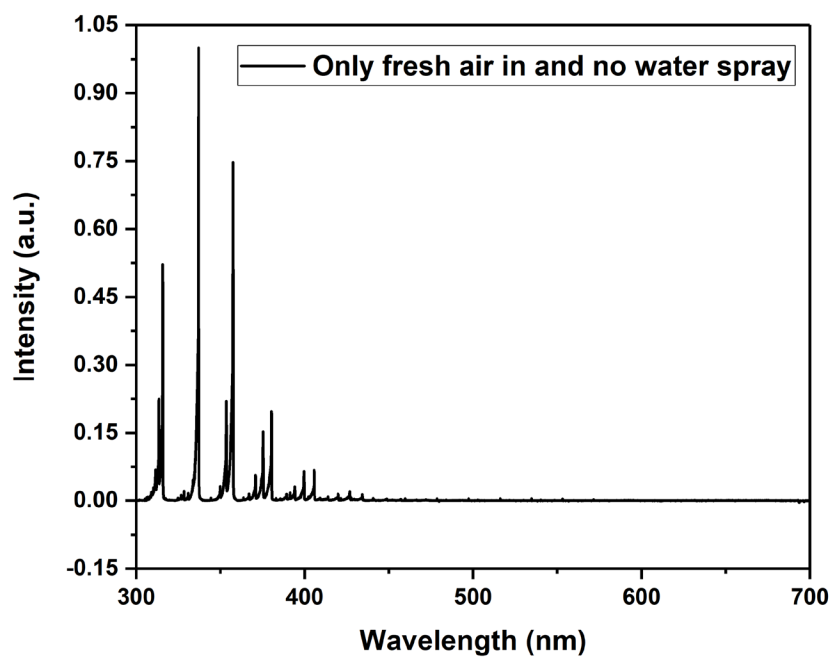
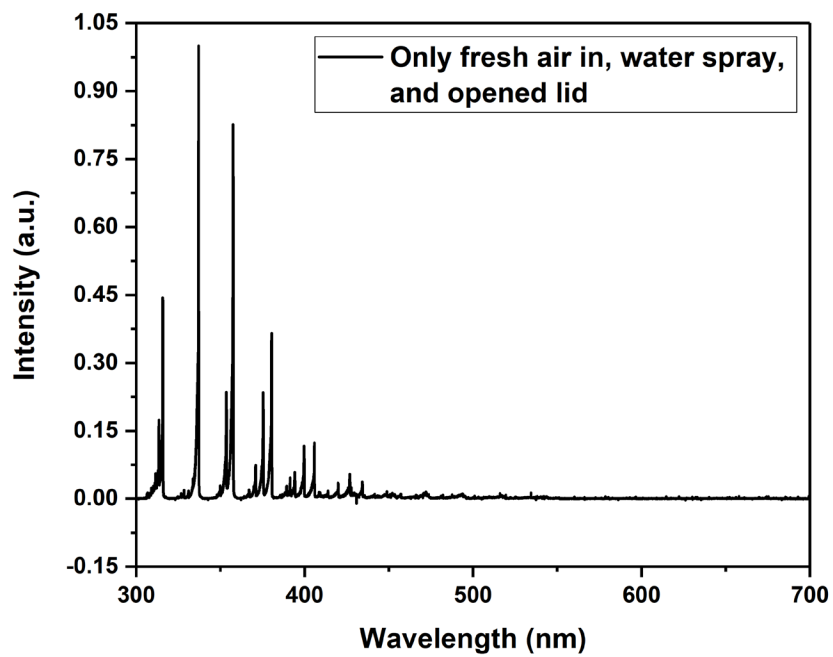
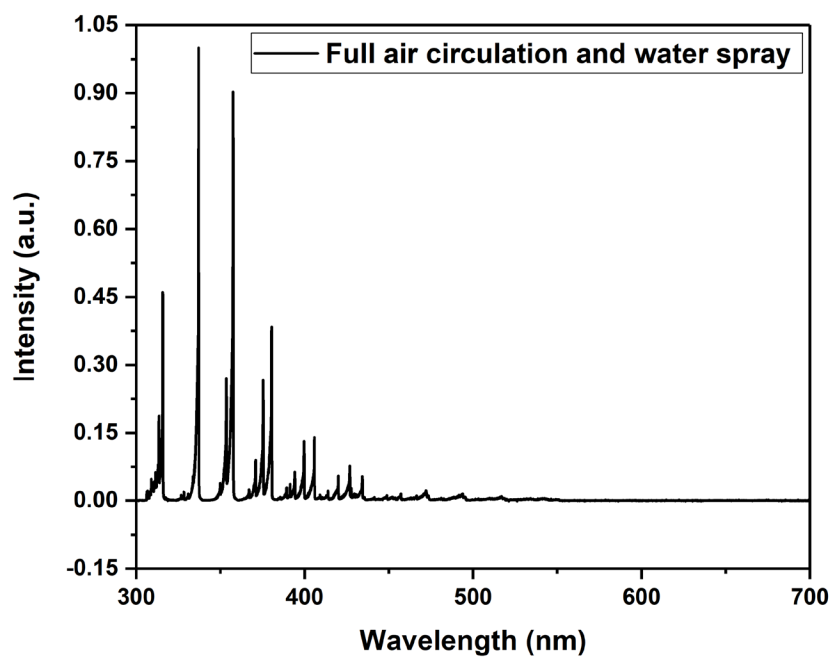


Figure 3.17: continued.



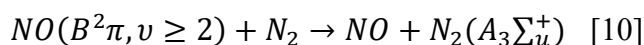
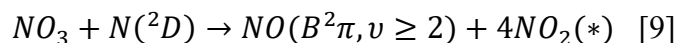
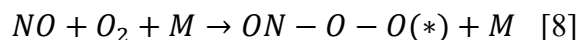
### 3.7.4 RF plasma temperatures calculation and possible reaction kinetics

Table 3.9 summarizes the relations between different experiment setups and three temperatures - electron temperature, rotational temperature, and vibrational temperature. From the table, the first thing that should be paid attention to is that all temperatures are much higher than what we got in DBD case. The additions of water spray, fresh air, or both will make all three temperatures decrease. It is quite intuitive since these additions will cool down the plasma region.

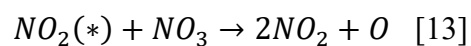
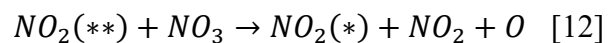
Table 3.9: Three temperatures under different experiment setups.

Experiment setup	Electron temperature, eV	Rotational temperature, K	Vibrational temperature, K
No air flow and no water spray	10.5	1000	3700
Only fresh air in and no water spray	4.07	850	3300
Full air circulation and no water spray	5.74	950	3600
Full air circulation and water spray	4.93	920	3400
Only fresh air in, water spray, and opened lid	4.01	700	3250

According to section 3.6.4, for DBD treatments, the higher the rotational temperature is, the lower the energy efficiency will be, and the more nitrite ions will be produced. For RF plasma treatments, the lowest rotational temperature we achieved is almost twice higher than the highest value we got in DBD case (500 K for 2000 Hz PRF), let alone the actual experimental setup which will lead to a rotational temperature of 920 K. However, the energy consumption per one nitrate ion is the lowest in RF plasma. The productivity is impressive, and the nitrite concentration is low enough to be negligible. Our hypothesis is that the extremely high rotational temperatures will activate secondary reactions:



In reaction [10], a large amount of  $NO$  and  $N_2(A_3\Sigma_u^+)$  will be produced. The latter one will compensate for the same molecules consumed in reactions [5] and [6] and reaction [4] is back online. More nitric oxide will be produced and reaction [8] is further promoted.  $NO$  could then join the following reactions:



With water, the nitrogen dioxide will produce nitrate and nitric oxide. But in our case, the oxygen is abundant. So only nitrate ions are our final product.

## CHAPTER 4. CONCLUSIONS AND FUTURE WORKS

### 4.1 Summary of all experiment results

Table 4.1 summarizes the maximum nitrate concentrations and the minimum energy consumptions per one nitrate ion that we can achieve with different kinds of discharges. The length of treatment time and the maximum water volume are also listed. To compare, we measured nitrate concentrations for water samples collected from Wabash river and our lab's tap water faucet. Simply based on the nitrate concentration, one can tell that the atmospheric arc discharge, DC positive corona discharge, DC voltage driven cold plasma torch, and even DBD are not feasible options to produce liquid fertilizers on large scale since even the nitrate concentration of Wabash river is much higher than those of water treated with these four plasma sources. RF plasma seems like the only option for us.

Table 4.1: Summary of results for all plasma sources and comparison with two water sources.

Plasma source	Treatment time, s	Water volume, mL	Final nitrate concentration, mg/L	Energy consumption per one nitrate ion, eV
Atmospheric pressure arc discharge	60	200	25	7800
Atmospheric pressure DC positive corona discharge (pin to water)	3000	10	6	4100
DC voltage driven cold plasma torch operating with helium	3600	10	3.5	690
DBD (30 Hz)	3600	10	24	500
RF plasma	86400	4000	1000	390
Wabash river	-	-	30	-
Lab tap water (not fixed)	-	-	7	-

#### 4.2 Atmospheric pressure high temperature arc plasma system

This type of plasma was employed as a fertilizer production source for our first experiment and efficiency of this process was calculated. It turned out that, in comparison to existing chemical processes (Harbor-Bosch Process is in the magnitude of tens of eVs), this method is exceedingly ineffective, not to mention the limited productivity due to the rapidly consumed electrodes. The major part of energy consumption happens in the heating process of water and ambient air. Moreover, and again, because of the very high-temperature arc, like what happened in a typical welding job, we observed fast disruption of the HV electrode. To summarize, we believe that atmospheric pressure high-temperature equilibrium arc plasma is unpromising for low-cost nitrogen fertilizer production. Nonequilibrium plasma, where ions' and molecules' temperatures are about the room temperature, looks more reasonable.

#### 4.3 Atmospheric pressure DC positive corona discharge

In comparison with a high temperature arc, the DC positive corona discharge is much less powerful. It is required to treat water for up to thousands of seconds to achieve a measurable nitrate ion concentration. In order to reduce the length of treatment time, one could employ high voltage pins. However, this will require additional experiment to find out the setup which maximizes the production efficiency. Moreover, the water after treatment showed acidic property ( $\text{pH} < 7$ ), which is not desirable for direct applying to plants. Energy cost per one nitrate ion is around a half of that for the arc system. Still, this is an unfavorable number for any commercial application. Also, to get this energy efficiency, one has to develop a special high voltage DC power supply with efficiency around 80-90 percent.

The corona current profile led us to study the pulsed corona discharge. Under the assumption that the primary contribution to the ion production is from pulses, by eliminating the DC permanent current component, we get five times less energy costs per one ion.

#### 4.4 DC voltage driven cold plasma torch operating with helium

This “corona like” plasma source has a very similar current profile: a permanent DC component and a pulsed component. Both components in this cold plasma torch are lower than that will be observed in a typical corona discharge. It leads to less energy consumption with just measurable nitrate concentration. From the other side, the energy costs are still higher than values produced by other research groups. Again, the productivity is way too low. This plasma source is still infeasible to our fertilizer project.

#### 4.5 Atmospheric pressure dielectric barrier discharge system

Atmospheric pressure DBD is a more feasible option than the above three plasma sources. We managed to get 24 mg/L in 10 mL water and 500 mg/L in 500 mL water. The treatment time is an hour and the energy efficiency is below 1000 eV per one nitrate ion. It should be noted that the

amount of energy stored in one HV pulse is about ten times more than the combination of energy going from this pulse into the plasma and other power dissipating in coaxial cables and the HV pulser. We employed the optical emission spectroscopy to study reaction kinetics of this plasma source. One major finding is that the lower the rotational temperature is, the higher the energy efficiency will be. One possible reaction kinetic is purposed.

#### 4.6 Atmospheric pressure radio frequency plasma system

So far, the atmospheric pressure RF plasma is the most feasible plasma source for this fertilizer project. We can achieve 1000 mg/L in 4 L water. The treatment time is 24 hours and the energy consumption per one nitrate ion is about 390 eV. We also employed the optical emission spectroscopy to this plasma source and based on the obtained spectrums, a secondary reaction is purposed.

#### 4.7 Future works

One possible future work is to employ residual gas analyzer (RGA) to verify our purposed reaction kinetics in DBD and RF plasma. Also, we can know exact gas compositions inside the treatment chambers. Better knowledge of reaction kinetics of these plasma sources can help us design novel experiment setups and further reduce energy consumption per one nitrate ion.

From the side of pure science, we could try discharges with low pressures (several Torr). This condition may help us achieve an even lower energy consumption per one nitrate ion. Tens-of-eVs energy consumption is expected. Micro plasma is also a novel idea to try. The nitrate ion synthesis efficiency might be higher on a small scale and thus, the energy consumption per one nitrate ion could be reduced.

The third one is to design solar powered local fertilizer production factory. This idea is beneficial for remote areas such as poor countries in Africa. We can do a simple calculation with the information listed on Table 4.2:

Table 4.2: Estimation for solar powered local fertilizer production factory located in Kenya.

Parameter	Value
Nitrogen (N) needed for corn	50 kg/year/ha
Ave. photovoltaic power potential in Kenya (max 1850) - $E_{year}$	1650 kWh/m <sup>2</sup>
One ion cost - $E_0$	390 eV or $6.2e^{-17}$ J
Solar panel efficiency - $\eta_1$	20%
Electrical conversion efficiency - $\eta_2$	80%

The below formula is used to calculate the square meter we have to occupy to mount solar panels which will provide power to fertilizer production factory to produce liquid nitrate fertilizer for 1-hectare corn farm, where  $\mu$  is the molar mass of the nitrogen atom and  $N_A$  is the Avogadro Constant:

$$m = \mu * v = \mu * \frac{N}{N_A} = \mu * \frac{1}{N_A} * \frac{E_{year} * \eta_1 \eta_2}{E_0} = 0.36 \left( \frac{kg}{m^2 year} \right)$$

Thus, we need only 139 m<sup>2</sup> of solar panels, or less than 1.5% of the total farm area to be covered with solar panels. Besides, we cooperate with the department of agriculture at Purdue University. They carried out several field tests to compare our liquid fertilizer with traditional ammonia fertilizers. The plants' growth data show that our liquid nitrate fertilizer is comparable to traditional fertilizers. This conclusion proves the feasibility of building solar powered local fertilizer production factory.

## REFERENCES

1. Galloway, James N., and Ellis B. Cowling. "Reactive nitrogen and the world: 200 years of change." *AMBIO: A Journal of the Human Environment* 31.2 (2002): 64-71.
2. Smil, Vaclav. *Enriching the earth: Fritz Haber, Carl Bosch, and the transformation of world food production*. MIT press, 2004.
3. "International Energy Outlook 2018". U.S. Energy Information Administration. Available at: [https://www.eia.gov/outlooks/ieo/pdf/executive\\_summary.pdf](https://www.eia.gov/outlooks/ieo/pdf/executive_summary.pdf).
4. Fertilizer statistics. "Raw material reserves". International Fertilizer Industry Association. Archived from the original on 24 April 2008. Available at: <https://www.fertilizer.org/404.aspx?aspxerrorpath=/iMIS2/404.aspx>.
5. Smith, Barry E. "Nitrogenase reveals its inner secrets." *Science* 297.5587 (2002): 1654-1655.
6. Rafiqul, Islam, et al. "Energy efficiency improvements in ammonia production-perspectives and uncertainties." *Energy* 30.13 (2005): 2487-2504.
7. International Energy Agency-IEA. *Technology Roadmap: Energy and GHG Reductions in the Chemical Industry via Catalytic Processes*, 2013, 1–55. Available at: <https://www.iea.org/publications/freepublications/publication/technology-roadmap-energy-and-ghgreductions-in-the-chemical-industry-via-catalytic-processes.html>.

8. Patil, B. S., et al. "Plasma assisted nitrogen fixation reactions." *Alternative Energy Sources for Green Chemistry*. Cambridge, UK: Royal Society of Chemistry, 2016. 296-338.
9. Lan, Rong, John TS Irvine, and Shanwen Tao. "Ammonia and related chemicals as potential indirect hydrogen storage materials." *International Journal of Hydrogen Energy* 37.2 (2012): 1482-1494.
10. Sivachandiran, L., and A. Khacef. "Enhanced seed germination and plant growth by atmospheric pressure cold air plasma: combined effect of seed and water treatment." *RSC Advances* 7.4 (2017): 1822-1832.
11. Randeniya, Lakshman K., and Gerard JJB de Groot. "Non - Thermal Plasma Treatment of Agricultural Seeds for Stimulation of Germination, Removal of Surface Contamination and Other Benefits: A Review." *Plasma Processes and Polymers* 12.7 (2015): 608-623.
12. Fridman, A., A. Chirokov, and A. Gutsol. "Non-thermal atmospheric pressure discharges." *Journal of Physics D: Applied Physics* 38.2 (2005): R1.
13. Burlica, R., K-Y. Shih, and B. R. Locke. "Formation of H<sub>2</sub> and H<sub>2</sub>O<sub>2</sub> in a water-spray gliding arc nonthermal plasma reactor." *Industrial & Engineering Chemistry Research* 49.14 (2010): 6342-6349.
14. Liang, Chenghong, Yaoting Jiang, and Yunchuang Wang. "Discussion of application of corona field in sterilization of flour paste." *China Brewing* 10 (2010): 049.

15. Machala, Zdenko, Lenka Chládeková, and Michal Pelach. "Plasma agents in bio-decontamination by dc discharges in atmospheric air." *Journal of physics D: Applied physics* 43.22 (2010): 222001.
16. Sobacchi, M. G., et al. "Pulsed corona plasma technology for treating VOC emissions from pulp mills." TAPPI Paper Summit, Spring Technical and International Environmental Conference, Atlanta, GA, USA. 2004.
17. Staack, David, et al. "Nanoscale corona discharge in liquids, enabling nanosecond optical emission spectroscopy." *Angewandte Chemie* 120.42 (2008): 8140-8144.
18. Gibson, Katie, and Christine Haas. *Plasma assisted decontamination of biological and chemical agents*. Springer Science & Business Media, 2011.
19. Park, Dayonna P., et al. "Reactive nitrogen species produced in water by non-equilibrium plasma increase plant growth rate and nutritional yield." *Current Applied Physics* 13 (2013): S19-S29.
20. García - Reyes, Juan F., et al. "Direct olive oil analysis by low - temperature plasma (LTP) ambient ionization mass spectrometry." *Rapid Communications in Mass Spectrometry: An International Journal Devoted to the Rapid Dissemination of Up - to - the - Minute Research in Mass Spectrometry* 23.19 (2009): 3057-3062.
21. Locke, B. R., et al. "Electrohydraulic discharge and nonthermal plasma for water treatment." *Industrial & engineering chemistry research* 45.3 (2006): 882-905.

22. Vanraes, Patrick. Electrical discharge as water treatment technology for micropollutant decomposition. Diss. Ghent University, 2016.
23. Malik, Muhammad Arif. "Nitric oxide production by high voltage electrical discharges for medical uses: a review." *Plasma Chemistry and Plasma Processing* 36.3 (2016): 737-766.
24. Park, Dayonna P., et al. "Reactive nitrogen species produced in water by non-equilibrium plasma increase plant growth rate and nutritional yield." *Current Applied Physics* 13 (2013): S19-S29.
25. Patil, Bhaskar S., et al. "Plasma assisted nitrogen oxide production from air: Using pulsed powered gliding arc reactor for a containerized plant." *AIChE Journal* 64.2 (2018): 526-537.
26. Goldman, M., A. Goldman, and R. S. Sigmond. "The corona discharge, its properties and specific uses." *Pure and Applied Chemistry* 57.9 (1985): 1353-1362.
27. Clements, J. Sidney, Masayuki Sato, and Robert H. Davis. "Preliminary investigation of prebreakdown phenomena and chemical reactions using a pulsed high-voltage discharge in water." *IEEE Transactions on Industry Applications* 2 (1987): 224-235.
28. Brisset, J. L., et al. "Interactions with aqueous solutions of the air corona products." *Revue de Physique Appliquee* 25.6 (1990): 535-543.

29. Lelievre, J., N. Dubreuil, and J-L. Brisset. "Electrolysis processes in DC corona discharges in humid air." *Journal de Physique III* 5.4 (1995): 447-457.
30. Gibalov, Valentin I., and Gerhard J. Pietsch. "The development of dielectric barrier discharges in gas gaps and on surfaces." *Journal of Physics D: Applied Physics* 33.20 (2000): 2618.
31. Shainsky, Natalie, et al. "Retraction: plasma acid: water treated by dielectric barrier discharge." *Plasma processes and Polymers* 9.6 (2012).
32. Dockery, K. P., et al. "Surface acid chemistry associated with dielectric barrier discharge (DBD) treatment of polyethylene." *Plasma Sources Science and Technology* 16.1 (2006): 42.
33. Elsaadany, Mostafa, et al. "Exogenous nitric oxide (NO) generated by NO-plasma treatment modulates osteoprogenitor cells early differentiation." *Journal of Physics D: Applied Physics* 48.34 (2015): 345401.
34. Heuer, Kiara, et al. "The topical use of non-thermal dielectric barrier discharge (DBD): Nitric oxide related effects on human skin." *Nitric Oxide* 44 (2015): 52-60.
35. Laurita, R., et al. "Chemical analysis of reactive species and antimicrobial activity of water treated by nanosecond pulsed DBD air plasma." *Clinical Plasma Medicine* 3.2 (2015): 53-61.

36. Hu, Yingmei, et al. "Application of dielectric barrier discharge plasma for degradation and pathways of dimethoate in aqueous solution." *Separation and Purification Technology* 120 (2013): 191-197.
37. Feng, Jingwei, et al. "Degradation of aqueous 3, 4-dichloroaniline by a novel dielectric barrier discharge plasma reactor." *Environmental Science and Pollution Research* 22.6 (2015): 4447-4459.
38. Marotta, Ester, et al. "Advanced oxidation process for degradation of aqueous phenol in a dielectric barrier discharge reactor." *Plasma Processes and Polymers* 8.9 (2011): 867-875.
39. Schutze, Andreas, et al. "The atmospheric-pressure plasma jet: a review and comparison to other plasma sources." *IEEE transactions on plasma science* 26.6 (1998): 1685-1694.
40. Park, Jaeyoung, et al. "An atmospheric pressure plasma source." *Applied Physics Letters* 76.3 (2000): 288-290.
41. Moon, Se Youn, W. Choe, and B. K. Kang. "A uniform glow discharge plasma source at atmospheric pressure." *Applied Physics Letters* 84.2 (2004): 188-190.
42. Balcon, Nicolas, Ana Aanesland, and Rod Boswell. "Pulsed RF discharges, glow and filamentary mode at atmospheric pressure in argon." *Plasma Sources Science and Technology* 16.2 (2007): 217.

43. Smith, H. B., Christine Charles, and R. W. Boswell. "Breakdown behavior in radio-frequency argon discharges." *Physics of Plasmas* 10.3 (2003): 875-881.
44. Jeong, J. Y., et al. "Etching materials with an atmospheric-pressure plasma jet." *Plasma Sources Science and Technology* 7.3 (1998): 282.
45. Babayan, S. E., et al. "Deposition of silicon dioxide films with an atmospheric-pressure plasma jet." *Plasma Sources Science and Technology* 7.3 (1998): 286.
46. Zajíčková, L., et al. "Study of plasma polymerization from acetylene in pulsed rf discharges." *Thin Solid Films* 425.1-2 (2003): 72-84.
47. De Benedictis, S., and G. Dilecce. "Time resolved diagnostics for kinetic studies in N<sub>2</sub>/O<sub>2</sub> pulsed rf discharges." *Journal de Physique III* 6.9 (1996): 1189-1204.
48. Wang, Xingxing, and Alexey Shashurin. "Study of atmospheric pressure plasma jet parameters generated by DC voltage driven cold plasma source." *Journal of Applied Physics* 122.6 (2017): 063301.
49. Ley, Hood-Hong. "Analytical methods in plasma diagnostic by optical emission spectroscopy: A tutorial review." *Journal of Science and Technology* 6.1 (2014).
50. Wiese, Wolfgang L., and Jeffrey R. Fuhr. "Improved critical compilations of selected atomic transition probabilities for neutral and singly ionized carbon and nitrogen." *Journal of Physical and Chemical Reference Data* 36.4 (2007): 1287-1345.